
Lipschitz verification of neural networks through training

Simon Kuang¹ Yuezhu Xu² S. Sivaranjani² Xinfan Lin¹

Abstract

The global Lipschitz constant of a neural network governs both adversarial robustness and generalization. Conventional approaches to “certified training” typically follow a train-then-verify paradigm: they train a network and then attempt to bound its Lipschitz constant. Because the efficient “trivial bound” (the product of the layer-wise Lipschitz constants) is exponentially loose for arbitrary networks, these approaches must rely on computationally expensive techniques such as semidefinite programming, mixed-integer programming, or branch-and-bound. We propose a different paradigm: rather than designing complex verifiers for arbitrary networks, we design networks to be verifiable by the fast trivial bound. We show that directly penalizing the trivial bound during training forces it to become tight, thereby effectively regularizing the true Lipschitz constant. To achieve this, we identify three structural obstructions to a tight trivial bound (dead neurons, bias terms, and ill-conditioned weights) and introduce architectural mitigations, including a novel notion of norm-saturating polyactivations and bias-free sinusoidal layers. Our approach avoids the runtime complexity of advanced verification while achieving strong results: we train robust networks on MNIST with Lipschitz bounds that are small (orders of magnitude lower than comparable works) and tight (within 10% of the ground truth). The experimental results validate the theoretical guarantees, support the proposed mechanisms, and extend empirically to diverse activations and non-Euclidean norms.

1. Introduction

Some neural networks that minimize a loss function on training data are found to underperform on unseen inputs; others perform well on the whole population, but can be easily fooled by imperceptibly small adversarial perturbations. A network may elevate a small variation (sampling error, infinitesimal distribution shift) above true features in the data. A recent hypothesis (Szegedy et al., 2014) supported by learning theory (Bartlett et al., 2017; Neyshabur et al., 2015b; Golowich et al., 2018; Neyshabur et al., 2018) explains both failure modes in terms of the Lipschitz constant.

The Lipschitz constant, defined as the maximum change in output per unit change in input, is a nonnegative scalar that quantifies the network’s power to amplify and discriminate relevant features in the training population—a desirable trait—and its tendency to behave erratically on unseen or out-of-distribution inputs—an undesirable trait. It follows that the global Lipschitz constant ought to be simultaneously as large as necessary and as small as possible. This tradeoff has traditionally been captured in mathematical programming by the support vector machine and lasso (for linear models), and by regularized kernel methods (for low-dimensional nonlinear models).

The former objective of this tradeoff (as large as necessary) is easily captured by a loss function. The latter objective has proven more elusive. It stands to reason that before claiming that a network’s Lipschitz constant is small, we first need to find out its value. But the exact Lipschitz constant of a neural network is NP-hard to compute in general (Virmaux & Scaman, 2018), and algorithms are only known for piecewise linear activations such as ReLU (Jordan & Dimakis, 2020; Bhowmick et al., 2021).

Consequently, we must rely on upper bounds. A range of methods for upper-bounding the Lipschitz constant exploit information such as the monotonicity of the activation function or the compact ranges of hidden layers. These techniques include semidefinite programming (SDP) (Fazlyab et al., 2019; Xu & Sivaranjani, 2024; 2025), polynomial optimization (Chen et al., 2020), interval arithmetic (Zhang et al., 2018; 2019), and operations research methods (Entesari et al., 2023; Shi et al., 2025). These occupy a spectrum of tradeoffs between conservatism and runtime complexity.

¹Department of Mechanical and Aerospace Engineering, University of California, Davis ²Edwardson School of Industrial Engineering, Purdue University. Correspondence to: Simon Kuang <slku@ucdavis.edu>.

At one extreme, one can quickly bound the Lipschitz constant of the network by multiplying the Lipschitz constants of the layers (Virmaux & Scaman, 2018, Prop. 1); we denote this the *trivial bound* (after Xu & Sivaranjani 2024). *A priori*, the trivial bound appears to increase exponentially with network depth and is therefore liable to extreme conservatism (Szegedy et al., 2014; Weng et al., 2018; Leino et al., 2021). Experimental evidence for this thesis ranges from drastic— 10^2 (Zhang et al., 2018, Figure 3)—to galactic—in excess of 10^{20} (Fazlyab et al., 2019, Figure 2b).

There are several schools of thought on how to balance “as large as necessary” and “as small as possible.” Some works impose a hard Lipschitz constraint in training, either as a projection operator in the training loop (Xu & Sivaranjani, 2023; Revay et al., 2024; Gouk et al., 2021; Junnarkar et al., 2024) or by a parameterization whose range lies within the Lipschitz cylinder (Wang & Manchester, 2023). Other works promote Lipschitz continuity indirectly by adding a Lipschitz penalty to the loss function (Pauli et al., 2021; Bungert et al., 2021; Huang et al., 2021). All of these methods are computationally expensive and impose extra parameters, hyperparameters, mathematical programs, or subroutines because they access the Lipschitz constant via sophisticated techniques such as semidefinite programming. They assume that these techniques are necessary because the trivial bound is too loose for verification and therefore too restrictive for training. (We respond in detail to different versions of this argument in Appendix A.)

Our work challenges this popular assumption.

We admit that the trivial bound is unacceptably loose for a general neural network. But as we show in Section 3.2, so is the SDP bound. Because “verifying robustness for arbitrary neural networks is hard,” Raghunathan et al. (2018) call for training “neural networks that are amenable to verification, in the same way that it is possible to write programs that can be formally verified.”

Surprisingly, the trivial bound is fit for this purpose. As we show by theory in Section 3.3 and example in Section 5, the trivial bound *becomes* tight when it is penalized in training. Lipschitz regularization then regulates the true Lipschitz constant of the network. Instead of designing the verification subtask for an arbitrary neural network, our approach is to design the network architecture and loss function in order to be verifiable by the trivial Lipschitz bound.

Related work (robustness) A small global Lipschitz constant guarantees that within a ball of radius inversely proportional to the Lipschitz constant, the classifier is indifferent to perturbations. Some other regularizers (Hoffman et al. 2019; Nenov et al. 2024; Yoshida & Miyato 2017, among others) impose a similar inductive bias towards smoothness, but do not come with a guarantee. Local Lipschitz bounds

(Jordan & Dimakis, 2020; Bhowmick et al., 2021; Xu & Sivaranjani, 2025) and other forms of robustness certificates (Raghunathan et al., 2018; Wong & Kolter, 2018; Lee et al., 2020) offer guarantees on a “pointwise,” per-instance basis by introspection of the network’s weights, given knowledge of the input and attack parameters. Rather, global Lipschitz bounds are “uniform” and apply to all inputs and all attacks, and impose a constant cost at inference time.

Contributions We attribute the looseness of the trivial bound to three causes: dead neurons, biases, and ill-conditioned weight matrices. We then mitigate them at the level of architecture and loss function (rather than overcome them in downstream analysis) with polyactivations, a novel vector-valued activation architecture designed to saturate norm bounds; sinusoidal activation layers that do not need biases to be universal approximators; and direct penalization of the trivial Lipschitz bound. We verify these mitigations and their theoretical backing experimentally on a range of networks and datasets (Iris, Section 5.1; MNIST, Section 5.2). Empirically, we find orders-of-magnitude improvements to the trivial bound that bring it to within a factor of 1–2 of the true Lipschitz constant. We also find support for the theoretical mechanisms behind these improvements, such as an argument by matrix factorization that Lipschitz regularization leads to well-conditioned matrices. We show that these empirical results translate to activation functions ranging from specialized to conventional, and to non-Euclidean norms.

We demonstrate the performance of this approach by training a neural network with cross-entropy loss to 98% on MNIST and certifying that its Lipschitz constant lies between 5.5 and 6. This is a remarkable achievement because:

1. It is relatively rare in the vast literature on Lipschitz analysis to ground-truth against lower bounds.¹
2. Our network’s Lipschitz upper bound is significantly smaller than other estimates for networks with comparable performance, whose Lipschitz upper bounds range from 50 to 500 (Fazlyab et al., 2019, Fig. 2a).
3. The training consists of minimizing a loss function (namely, a data loss plus the trivial Lipschitz bound) using a black-box first-order optimizer.
4. The verification method is likewise elementary: it consists of multiplying induced norms of weight matrices to obtain an upper bound, and locally searching for a secant vector that attains the Lipschitz constant to obtain a lower bound.

¹Wang & Manchester (2023) also compares to empirical lower bounds on a 1D toy problem. Jordan & Dimakis (2020); Bhowmick et al. (2021); Sbihi et al. (2024) compute lower bounds in super-polynomial time.

2. Preliminaries

The vector of ones is $\mathbf{1}$. The ℓ^p norm of $x \in \mathbb{R}^d$ is defined by

$$\|x\|_p = \left(\sum_{i=1}^d |x_i|^p \right)^{1/p}, \quad p \in [1, \infty);$$

$$\|x\|_\infty = \max_{i \in [d]} |x_i|, \quad p = \infty.$$

The induced operator p -norm of a matrix $A \in \mathbb{R}^{d \times d}$ is defined by

$$\|A\|_p = \max_{\|x\|_p=1} \|Ax\|_p.$$

The Lipschitz constant of an absolutely continuous function $f : \mathbb{R}^n \rightarrow \mathbb{R}^m$ in the p -norm is

$$\|f\|_{\text{Lip},p} = \sup_{x \in \mathbb{R}^n} \|\nabla f(x)\|_p.$$

We may omit the subscript when $p = 2$.

A traditional feed-forward neural network of depth L is defined recursively by $x^0 = x$ and

$$x^\ell = \sigma^\ell \left(W^\ell x^{\ell-1} + b^\ell \right), \quad \ell = 1, \dots, L, \quad (1)$$

where σ^ℓ acts elementwise and W^ℓ and b^ℓ are the weights and biases of layer ℓ . We write $f(x) = x^L$. Because induced matrix norms are submultiplicative, the **trivial bound** on the Lipschitz constant of a feed-forward network is

$$\|f\|_{\text{Lip},p} \leq \prod_{\ell=1}^L \left\| \sigma^\ell \right\|_{\text{Lip},p} \left\| W^\ell \right\|_p.$$

For $z \in \mathbb{R}^n$, define $\text{Sin}(z) = \text{diag}(\sin(z))$ and $\text{Cos}(z) = \text{diag}(\cos(z))$.

If A is a matrix, $\text{Diag}(A)$ is the diagonal matrix with the same diagonal entries as A and zeros elsewhere.

The condition number of a (rectangular) matrix is the ratio of its largest singular value to its smallest *nonzero* singular value.

3. Mitigating weaknesses of the trivial bound

This section presents a stylized narrative of three phenomena underlying the looseness of the trivial Lipschitz bound. For each phenomenon, we construct a toy model that inflates the trivial Lipschitz bound and propose an architecture- and/or loss-level mitigation motivated by theoretical analysis. The purpose is to advocate for a single gold-standard architecture for shallow networks—cosine/sine activations trained with a straightforward penalty on the trivial Lipschitz bound—and to raise questions for empirical investigation on deeper networks.

3.1. Dead neurons

Popular activation functions such as ReLU and hyperbolic tangent have regions with little variation. A ReLU preactivation h may be biased into its negative region across the entire training set; thus, a unit such as $\text{ReLU}(1000h)$ may become positive at test time (e.g., under distribution shift). In such a case, the unit’s Lipschitz constant is 1000, even though this steep slope may be irrelevant (or harmful) to out-of-sample performance.

Dead neurons can also result from deeper structures such as the mapping $x \mapsto z$ given by

$$z = \text{ReLU}(-1000y),$$

$$y = \text{ReLU}(1000x).$$

In this case, the trivial bound equals 1 million, but the true Lipschitz constant is 0, because the argument of the second layer’s ReLU is nonpositive for every x . In general, computing tight neuron ranges is computationally intractable (Weng et al., 2018; Shi et al., 2022; Jordan & Dimakis, 2020; Chen et al., 2020; Virmaux & Scaman, 2018).

We mitigate this issue by using polyactivations that saturate the Lipschitz constraint without vanishing slopes.

3.1.1. POLYACTIVATIONS

Merely adding a residual bypass to a dead neuron is *not* sufficient from the perspective of the Lipschitz bound, since layer bounds $(1 + \|W\|_p)$ would lead to a trivial bound that grows exponentially in depth (Gouk et al., 2021).

Some existing work on Lipschitz training replaces neuron-level nonlinearities with whole-layer nonlinearities such as GroupSort, whose Jacobian is orthogonal everywhere on its domain (Anil et al., 2019).² Our approach is closer to CReLU, which maps each input coordinate through multiple activations, ensuring that not all channels vanish simultaneously (Shang et al., 2016).

Definition 3.1 (Polyactivation). A polyactivation function of order K is a tuple of functions $\{\sigma_k : \mathbb{R} \rightarrow \mathbb{R}\}_{k=1}^K$ that acts on vectors by

$$\vec{\sigma} : \mathbb{R}^d \rightarrow \mathbb{R}^{dK},$$

$$x \mapsto (\sigma_1(x), \sigma_2(x), \dots, \sigma_K(x)).$$

Polyactivations fan out by a factor of K and are contracted by a wide weight matrix.³ The Jacobian of a polyactivation

²We note in passing that the neuron-level absolute value activation function also possesses this property.

³As the contribution of any neuron to the next layer’s neurons is a weighted sum of basis functions, this architecture can be recognized as a Kolmogorov-Arnold expansion (Liu et al., 2025).

layer is

$$\frac{\partial}{\partial x} \vec{\sigma}(x) = \begin{pmatrix} \text{diag } \sigma'_1(x) \\ \text{diag } \sigma'_2(x) \\ \vdots \\ \text{diag } \sigma'_K(x) \end{pmatrix} \in \mathbb{R}^{dK \times d}.$$

Next we formalize a notion under which a polyactivation function is ‘‘maximally’’ Lipschitz in the p -norm.

Definition 3.2 (Saturated polyactivation). A polyactivation function $\{\sigma_k\}_{k=1}^K$ is Lipschitz-saturated in the p -norm if $\vec{\sigma}$ has local Lipschitz constant 1 in every neighborhood of \mathbb{R}^d , or equivalently, for almost every $x \in \mathbb{R}$,

$$\begin{aligned} \sum_{k=1}^K |\sigma'_k(x)|^p &= 1, & \text{if } p \in [1, \infty); \\ \forall k \in [K], \quad |\sigma'_k(x)| &= 1, & \text{if } p = \infty. \end{aligned}$$

A saturated polyactivation is evidently strictly more expressive than a single activation function, as it can represent a richer class of functions while maintaining the same Lipschitz constraint. The idea of saturated polyactivations is to maximize the overall representational power while maintaining control over the Lipschitz bound.

Example 1. The absolute value activation function $x \mapsto |x|$ is a first-order polyactivation that saturates the p -norm Lipschitz constant for all $p \in [1, \infty]$.

Example 2. The ReLU activation $x \mapsto \max(0, x)$ is not saturated because its derivative is either 0 or 1. However, the CReLU (Shang et al., 2016) $x \mapsto (\max(0, x), \max(0, -x))$ is a second-order polyactivation that saturates the Lipschitz bound for $p \in [1, \infty)$. A variation that saturates the ∞ -norm Lipschitz constant is $x \mapsto (x, |x|)$.

Example 3. The hyperbolic tangent activation function can be augmented to saturate the 1-norm Lipschitz constant by the second-order polyactivation

$$x \mapsto (x, x - \tanh(x))$$

To saturate the 2-norm Lipschitz constant, one could opt for the third-order polyactivation $x \mapsto (\tanh(x), \text{sech}(x), \log \cosh(x))$.

Example 4. The sine activation function can be augmented to saturate the 2-norm Lipschitz constant by the second-order polyactivation $x \mapsto (\cos x, \sin x)$.

3.2. Biases

Equation (1) is not the only way to write the composition

$$\begin{aligned} &\text{activation}_{\sigma^\ell} \circ \text{shift}_{b^\ell} \circ \text{linear}_{W^\ell} \\ &\circ \text{activation}_{\sigma^{\ell-1}} \circ \text{shift}_{b^{\ell-1}} \circ \text{linear}_{W^{\ell-1}} \circ \dots \end{aligned}$$

where activation denotes the elementwise activation, shift denotes translation by the bias, and linear denotes matrix multiplication by the weights. Taking circular permutations, we see that there are three ways to associate these operations:

$$\text{activation} \circ \text{shift} \circ \text{linear}, \quad (\text{ASL})$$

$$\text{shift} \circ \text{linear} \circ \text{activation}, \quad \text{and} \quad (\text{SLA})$$

$$\text{linear} \circ \text{activation} \circ \text{shift}. \quad (\text{LAS})$$

Theorem 3.3. The trivial Lipschitz bound in the p -norm is tight for ASL units with generic $W \in \mathbb{R}^{d \times d}$ and $b \in \mathbb{R}^d$, and for SLA and LAS units with arbitrary $W \in \mathbb{R}^{d \times d}$ and $b \in \mathbb{R}^d$.

However, if we consider the quadruple composition

$$\text{linear} \circ \text{activation} \circ \text{shift} \circ \text{linear}, \quad (\text{LASL})$$

then the trivial Lipschitz bound in the p -norm can be seen to be arbitrarily loose for LASL units $x \mapsto W^1 \sigma(W^0 x + b)$, as we see from three different explicit constructions. The case of LASL is interesting because it is the prototypical multilayer perceptron used in the classical proof of universal approximation by approximate identities.

Theorem 3.4. For both the ReLU and tanh activation functions, there exist LASL units $\mathbb{R} \rightarrow \mathbb{R}^d \rightarrow \mathbb{R}$ on which the trivial 2-Lipschitz bound is $\Omega(d)$, but the true 2-Lipschitz constant ranges from $O(1)$ to $\Omega(d)$ by varying only the biases.

Theorem 3.5. For the sin activation function, there exist LASL units $\mathbb{R} \rightarrow \mathbb{R}^{2d} \rightarrow \mathbb{R}$ on which the trivial Lipschitz bound is $\Omega(d)$, but the true Lipschitz constant is 0.

Remark 3.6. These constructions show that not only the trivial bound, but also any Lipschitz bound which ignores the biases cannot help but impute to the biases their worst-case values, and is therefore liable to up to $\Omega(d)$ conservatism per layer on ReLU and tanh networks, and infinite conservatism on sinusoidal networks. (Fazlyab et al., 2019; Virmaux & Scaman, 2018; Xu & Sivaranjani, 2024).

We mitigate this issue by using a specific polyactivation structure that allows biases to be analytically absorbed into the weight matrices, thereby preventing the cancellation that loosens the bound.

3.2.1. RECTANGULAR SINUSOIDAL LAYERS

In §3.2, we saw that the trivial bound can be loose because biases in an LASL unit can induce cancellation. What can be done? Removing the shift parameter from LASL units would eliminate some slack in the trivial bound, but at the expense of universal approximation.

The criterion for mitigating this weakness is a dimension-independent guarantee that the bound can be sharp for LASL

units. We contribute such a guarantee in the 2-norm using the (\cos, \sin) polyactivation. Let a LASL unit $\mathbb{R}^r \rightarrow \mathbb{R}^n \rightarrow \mathbb{R}^m$ be defined by

$$x \mapsto A \cos(Wx + b) + B \sin(Wx + b),$$

where $A, B \in \mathbb{R}^{m \times n}$, $W \in \mathbb{R}^{n \times r}$, and $b \in \mathbb{R}^n$.

The key observation is that we can set $b = 0$ by absorbing the bias into the weight matrices via trigonometric identities (recall that $\text{Sin}(z) = \text{diag}(\sin(z))$ and $\text{Cos}(z) = \text{diag}(\cos(z))$):

$$\begin{aligned} A &\mapsto A \text{Cos}(b) - B \text{Sin}(b) \\ B &\mapsto A \text{Sin}(b) + B \text{Cos}(b) \end{aligned}$$

This immediately rules out the adversarial biasing in Theorem 3.5, which relied on the identity $\sin x + \sin(x + \pi) = 0$. Now the LASL unit becomes

$$x \mapsto A \cos(Wx) + B \sin(Wx), \quad (2)$$

and its trivial Lipschitz bound in the 2-norm is

$$\left\| \begin{pmatrix} A & B \end{pmatrix} \right\|_2 \|W\|_2. \quad (3)$$

3.3. Ill-conditioned weight matrices

A network with ill-conditioned weight matrices can be less Lipschitz than it appears. This occurs when a neural network contains ill-conditioned subnetworks that cancel out. Owing to the universal approximation property of neural networks, it suffices to make the point using two toy examples: the ReLU and linear activation functions.

The ReLU activation function is 1-homogeneous: for all $\alpha \in \mathbb{R}^x$, $\text{ReLU}(\alpha x) = \alpha \text{ReLU}(x)$. This means that if Λ is an invertible diagonal matrix, then any two consecutive layers can be reparameterized $(W^0, W^1) \mapsto (\Lambda^{-1}W^0, W^1\Lambda)$, while the composite function

$$\begin{aligned} W^1 \text{ReLU}(W^0 x + b^0) + b^1 \\ = W^1 \Lambda \text{ReLU}(\Lambda^{-1}W^0 x + \Lambda^{-1}b^0) + b^1 \end{aligned}$$

remains unchanged; this fact has been applied in another context to improve the training of ReLU networks (Neyshabur et al., 2015a; 2016). Given generic weight matrices W^0, W^1 , reparameterization by

$$\Lambda = \text{diag}(\lambda, 1, 1, 1, \dots), \quad \lambda \rightarrow \infty$$

results in a trivial Lipschitz bound of $\Theta(\lambda)$ times the original Lipschitz constant. (The weight matrices' condition number is also $\Theta(\lambda)$.) This form of ill-conditioning also evades analysis methods such as LipSDP-Layer (Fazlyab et al., 2019), which do not know the homogeneity of ReLU. We record this observation as:

Theorem 3.7. *Given any ReLU network, there exists a closed-form, mathematically equivalent network whose trivial 2-norm Lipschitz bound is arbitrarily large.*

It is easy to devise examples which make the trivial 2-norm Lipschitz bound look bad. That does not mean it is always bad.

Next, let us consider the problem of learning an invertible linear function as a deep neural network with *linear* activation function $\sigma(x) = x$. This is a partly linearized (Nam et al., 2025) model of an overparameterized deep network.

Without loss of generality, the objective is to learn the identity function using the mapping

$$x \mapsto W_L W_{L-1} \cdots W_1 x \quad (4)$$

where the parameters W_1, W_2, \dots, W_L are square matrices.

Theorem 3.8. *Consider a deep network (4) with linear activations and parameter matrices constrained by $W_L W_{L-1} \cdots W_1 = I$. Let $K = \|W_1\|_2 \|W_2\|_2 \cdots \|W_L\|_2$ be the trivial Lipschitz bound. Then the following are equivalent:*

1. $K = 1$, i.e. there is no conservatism in the trivial bound.
2. W_1, W_2, \dots, W_L minimize K subject to $W_L W_{L-1} \cdots W_1 = I$.
3. The condition number of each parameter matrix is 1.

In this toy example, minimizing the trivial Lipschitz bound over unconstrained degrees of freedom on a level set of the loss function recovers the ground truth Lipschitz constant.

3.3.1. LIPSCHITZ PENALTY

Plausibly, this principle generalizes to nonlinear σ and would suggest that well-conditioned neural parameterizations on which the trivial bound is tight can be reached by continuous optimization, which is hard in theory and easy in practice.

Therefore, we propose to train networks onto the Pareto frontier of low loss and low trivial Lipschitz bound, by choosing polyactivations that saturate the p -norm and solving a penalized optimization problem such as

$$\underset{\{W^\ell\}_{\ell=1}^L}{\text{minimize}} \quad \ell(W^1, \dots, W^L) + \lambda \prod_{\ell=1}^L \|W^\ell\|_p,$$

where ℓ is a data loss function such as negative log-likelihood over the training set and $\lambda > 0$ is a tuning parameter.

4. Theoretical and practical lower bounds

The literature on Lipschitz constant verification of neural networks uses “tightness” to refer to metrics such as the ratio of the global Lipschitz constant to the trivial bound (Fazlyab et al., 2019; Xu & Sivaranjani, 2024). But in the plain mathematical sense, a tight upper bound must be close to the ground truth. Because it is intractable to compute the true Lipschitz constant, we instead compute lower bounds and use the inequality

$$\begin{aligned} 1 \leq \text{tightness} &= \frac{\text{Lipschitz upper bound}}{\text{Lipschitz ground truth}} \\ &\leq \frac{\text{Lipschitz upper bound}}{\text{Lipschitz lower bound}} \end{aligned}$$

to show that our Lipschitz upper bounds, in spite of their simplicity, are effective approximations of the ground truth.

When considering only a LASL unit equipped with (\cos, \sin) and absolute value activations, we can derive lower bounds by proving that the Jacobian of the network is large “on average.” (Theorem B.1 advances a similar claim for the absolute value activation.)

Theorem 4.1 (Lower bound on sinusoidal networks). *Let $f(x)$ be an LASL unit from $\mathbb{R}^n \rightarrow \mathbb{R}^n \rightarrow \mathbb{R}^m$ given by Equation (2),*

$$f(x) = A \cos(Wx) + B \sin(Wx).$$

Then, if W has full rank, the following Lipschitz lower bound holds:

$$\begin{aligned} &\|f\|_{\text{Lip},2}^2 \\ &\geq \frac{1}{2} \lambda_{\max} [A \text{Diag}(WW^\top) A^\top + B \text{Diag}(WW^\top) B^\top], \end{aligned}$$

and the trivial Lipschitz bound

$$K = \left\| \begin{pmatrix} A & B \end{pmatrix} \right\|_2 \|W\|_2$$

is off by less than a factor of $\sqrt{2} \kappa(W)$:

$$\frac{1}{\sqrt{2} \kappa(W)} K \leq \|f\|_{\text{Lip},2} \leq K,$$

where $\kappa(W) = \sqrt{\lambda_{\max}(WW^\top)/\lambda_{\min}(WW^\top)}$ is the condition number.

The proof appeals to the probabilistic method to find an input with a typical Jacobian norm. A key cancellation step uses the fact that because these activations have slopes ranging from -1 to 1; a similar method would not work for ReLU or tanh (0 to 1).

In deeper networks, it is harder to get a lower bound on the Jacobian. However, we can still use the probabilistic

method over an ensemble of random networks to calculate the exact second moment of the Jacobian. This is weaker in that it is an average-case bound and only applies to the random initialization (which is quickly departed in training), but it is strong in that it holds with equality, pointwise in x .

The **random-phase initialization** of $(A, B) \in \mathbb{R}^{d \times d'}$ at scale α is defined as

$$\begin{pmatrix} A & B \end{pmatrix} = \begin{pmatrix} \bar{A} & \bar{B} \end{pmatrix} \begin{pmatrix} \cos(\theta) & -\sin(\theta) \\ \sin(\theta) & \cos(\theta) \end{pmatrix}, \quad (5)$$

where $\bar{A}, \bar{B} \in \mathbb{R}^{d \times d'}$ are i.i.d. Gaussian with variance α/d' , and θ is uniformly distributed on the torus $(\mathbb{R}/2\pi\mathbb{Z})^d$.

Informal Theorem (Theorem B.2). *Let f be a (\cos, \sin) neural network of depth L and arbitrary width, initialized with random phases at scale α .*

$$\mathbb{E}(Df(x)Df(x)^\top) = \alpha^L I$$

for every input x .

The idea of this proof is that the random phases⁴ decorrelate the weights across layers, leading to a diagonal covariance structure.

As a by-product, we have also established an *exact* stable initialization for sinusoidal networks (Sitzmann et al., 2020). The choice $\alpha = 1$ stabilizes the average slope of the network; the choice $\alpha = 2^{-1/2}$ corresponding to the Kaiming initialization stabilizes the worst case (He et al., 2015). This discrepancy reflects that at initialization, the trivial Lipschitz constant is loose by a factor of $\sqrt{2}$ per layer; it is the role of training to close this gap.

4.1. An empirical bound

In experiments, we obtain an empirical lower bound \hat{L} by locally maximizing the secant slope

$$\|f\|_{\text{Lip},2} \leq \hat{L} \approx \max_{x,y} \frac{\|f(x) - f(y)\|_2}{\|x - y\|_2 + \epsilon},$$

using $\epsilon = 10^{-8}$ and reporting the best of twenty runs of L-BFGS, initialized with x and y sampled from the training data. It is fitting that the network’s highest local variation should be attained on a line segment between training points, where the data loss function opposes the downward pressure on the Jacobian imposed by Lipschitz regularization.

5. Experimental results

We carry out numerical experiments at varying scales to address the following questions, which are left unresolved by our theoretical analysis.

⁴The random phases, which anti-correlate the fourth moments of the weights while leaving the second moments unchanged, do not have noticeable consequences for practical training.

Table 5.1. Iris experiment: final predictive performance after 20,000 steps.

λ	Train Loss	Test Loss	Train Acc.	Test Acc.
0	1.0×10^{-4}	0.4661	1.000	0.933
10^{-2}	0.0542	0.0932	0.983	0.967

Question 1 (Feasibility). *What is the effect of Lipschitz regularization on the trivial bound?*

Question 2 (Tightness). *What is the effect of Lipschitz regularization on the true Lipschitz constant?*

Question 3 (Performance). *What is the effect of Lipschitz regularization on the model’s goodness of fit, both in-sample and out-of-sample?*

Question 4 (Robustness). *How confidently does global Lipschitz regularization certify robust learning?*

5.1. Iris dataset: upper and lower 2-norm Lipschitz bounds on a shallow network

This section trains and evaluates a small multilayer perceptron (detailed in Section C.1) with (\cos, \sin) polyactivation on the Iris dataset in order to validate Theorem 4.1. We optimize the penalized objective $\text{NLL} + \lambda K$ for $\lambda \in \{0, 10^{-2}\}$.

To assess tightness, we compare K to (i) the guaranteed lower bound

$$\frac{K}{\sqrt{2}\kappa(W)} \leq \|f\|_{\text{Lip},2} \leq K,$$

and (ii) the empirical lower bound \widehat{L} .

Results While $\lambda = 0$ results in an exploding K , adding the Lipschitz penalty reduces K by more than an order of magnitude (Table 5.2, Question 1). Regularization also makes the trivial bound essentially tight in practice (Table 5.2, Question 2). Moreover, the Lipschitz upper bound ($K = 5.84$) of the regularized network is much smaller than the Lipschitz lower bound of the unregularized network ($\widehat{L} = 105.74$), indicating that the Lipschitz penalty reduces the network’s true Lipschitz constant.

While $\lambda = 0$ yields near-perfect interpolation and classical overfitting, adding the Lipschitz penalty improves test loss and slightly improves test accuracy (Table 5.1, answering Question 3).

Visually, on two-dimensional slices of the domain, the regularized network (Figure C.3) exhibits smoother boundaries than the unregularized network (Figure C.2).

5.2. MNIST dataset: Lipschitz bounds

This section trains and evaluates a larger network (detailed in Section C.3) on the MNIST dataset in order to validate the

Table 5.2. Iris experiment: 2-norm Lipschitz upper bound K versus lower bounds. Here $K/(\sqrt{2}\kappa(W))$ is the guaranteed lower bound from Theorem 4.1, while \widehat{L} is an empirical lower bound from local optimization of the Lipschitz ratio over input pairs.

λ	K (upper)	$K/(\sqrt{2}\kappa(W))$	\widehat{L}	K/\widehat{L}
0	179.21	25.04	105.74	1.69
10^{-2}	5.84	0.82	5.84	1.00

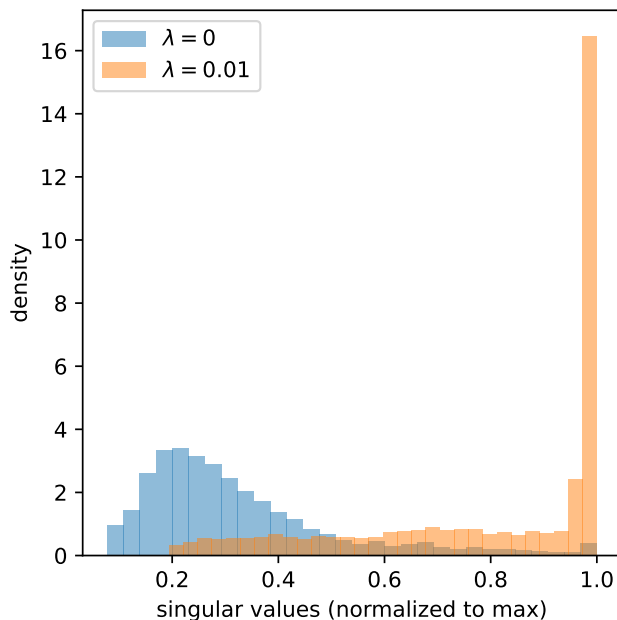


Figure 5.1. MNIST experiment: normalized singular values of the weight matrices (with and without penalty).

claim that the linearized Theorem 3.8 extends to nonlinear networks.

Results As with the Iris experiment, we find that $\lambda = 0$ results in an exploding Lipschitz upper bound, while adding a Lipschitz penalty leads to a reduction by one to two orders of magnitude (Table 5.3, Figure C.5, Question 1). We again run a local Lipschitz attack using L-BFGS to find a lower bound \widehat{L} on the global Lipschitz constant, and conclude (Table 5.3, Question 2):

1. Lipschitz regularization reduces the true Lipschitz constant of the resulting network by at least $\sim 10\times$, by comparing \widehat{L} of the unregularized network to K of the regularized network, and
2. The trivial Lipschitz upper bound K of the regularized network is conservative by no more than 10%, by comparing it to \widehat{L} of the same regularized network.

While the regularized network has a higher in-sample loss, it has comparable test error: 1.70% for $\lambda = 0$ versus 1.41%

Table 5.3. MNIST experiment: 2-norm Lipschitz upper bound K versus empirical lower bound \widehat{L} .

λ	K (upper)	\widehat{L} (lower)	K/\widehat{L}
0	187.32 ± 21.45	58.99 ± 3.79	3.18
10^{-2}	5.69 ± 0.03	5.18 ± 0.03	1.10

for $\lambda = 10^{-2}$ (Figure C.4, Question 3).

To quantify the effect on robustness (Question 4), we levy an ℓ_2 PGD attack on the MNIST test set using 40 projected gradient steps (step size $\epsilon/10$) for budgets $\epsilon \in \{2^{-1}, 2^{-2}, 2^{-3}, 2^{-4}, 2^{-5}\}$. The resulting adversarial error rates are reported in Table C.1 and plotted in Figure C.4. The Lipschitz-regularized model substantially reduces adversarial error at larger perturbation budgets (e.g., at $\epsilon = 2^{-1}$ the error drops from 13.04% to 4.90%). It also has tighter robustness certificates (obtained by comparing classification margin to perturbation budget times Lipschitz bound).

We also find empirical evidence for the mechanism modeled by Theorem 3.8. We plot the empirical distribution of all singular values of weight matrices, normalized by the maximum singular value of the same matrix, and find that the Lipschitz-regularized networks concentrate their singular value spectra near the maximum singular value (Figure 5.1). This supports the claim that penalizing the maximum singular value allows the optimizer to train the lower spectrum, to which the operator norm is indifferent.

Discussion: tightness In much of the literature on global Lipschitz verification of trained networks, a Lipschitz upper bound obtained by advanced methods is considered tight if it compares favorably to the trivial upper bound K (Fazlyab et al., 2019; Xu & Sivarajani, 2024). Unfortunately, this comparison is not ground-truthed against the true Lipschitz constant of the network. By contrast, our tightness ratio K/\widehat{L} upper-bounds the true conservatism of the trivial upper bound K . Our regularized MNIST network, like that of Xu & Sivarajani (2025), achieves $< 2\%$ test error when training with cross-entropy, but with a global Lipschitz upper bound of 5.69 (Table 5.3). This is commensurate with Xu & Sivarajani (2025)’s local Lipschitz certificates at a radius of 2^{-8} , and an order of magnitude smaller than Xu & Sivarajani (2025)’s local Lipschitz certificates at a radius of 2^{-1} .

Discussion: robustness We enter the quantitative “arms race” of robust learning (Raghunathan et al., 2018), with order-of-magnitude improvements in the Lipschitz constant. The robustness of our Lipschitz-regularized network against PGD attacks is comparable ($\pm 1\%$ at each attack radius) to that of Xu & Sivarajani (2025)’s MNIST network trained using a sophisticated local Jacobian penalty heuristic (Hoff-

man et al., 2019). The difference is that our method is a one-line algorithm with a single tuning parameter λ .

Comparisons with other methods Comparisons between our approach and other activation functions (Section D.1) and penalties (Section D.3), and extensions to other Lipschitz norms (Section D.2) are made in the appendix. In summary, we find that in deeper networks where Theorem 4.1 does not apply, the expressivity and tightness of our method result primarily from optimizing the trivial bound, with a smaller or ambivalent contribution from the choice of activation function. The absolute value activation often has the tightest bounds and best fit; ReLU the loosest bounds and worst fit. Across different settings, the mechanism of action seems to be that weight matrices are pushed to the corners of induced norm balls: well-conditioned matrices in the 2-norm, equal-row-norm matrices in the ∞ -norm, and equal-column-norm matrices in the 1-norm.

We also make an apples-to-apples comparison to direct parameterization, concluding that enforcing a hard Lipschitz constraint via a semidefinite program on a ReLU network is *more* restrictive than enforcing the same constraint via the trivial bound on an abs network (Section D.4).

6. Conclusion

We have shown that the trivial Lipschitz bound—the product of layerwise Lipschitz constants—can be made tight by design, rather than loose by default. We exploit overparameterization as an ally in this endeavor, as it provides the flexibility to optimize the trivial bound while maintaining expressivity. Our methodology does not require any new data structures, algorithms, or subroutines: it can be implemented as a single penalty term with a single hyperparameter.

By aligning the training objective with the verification method, we can obtain networks that are expressive, robust, and certifiable.

Impact Statement

This paper presents work whose goal is to advance the field of Machine Learning. There are many potential societal consequences of our work, none which we feel must be specifically highlighted here.

Reproducibility Statement

The results can be reproduced by running the Jupyter notebooks included in `lipschitz.zip`.

References

- Anil, C., Lucas, J., and Grosse, R. Sorting Out Lipschitz Function Approximation. In Chaudhuri, K. and Salakhutdinov, R. (eds.), *Proceedings of the 36th International Conference on Machine Learning*, volume 97 of *Proceedings of Machine Learning Research*, pp. 291–301. PMLR, June 2019.
- Bartlett, P. L., Foster, D. J., and Telgarsky, M. Spectrally-normalized margin bounds for neural networks. In *Proceedings of the 31st International Conference on Neural Information Processing Systems*, NIPS’17, pp. 6241–6250, Red Hook, NY, USA, 2017. Curran Associates Inc. ISBN 978-1-5108-6096-4. event-place: Long Beach, California, USA.
- Bhowmick, A., D’Souza, M., and Raghavan, G. S. LipBaB: Computing Exact Lipschitz Constant of ReLU Networks. In Farkaš, I., Masulli, P., Otte, S., and Wermter, S. (eds.), *Artificial Neural Networks and Machine Learning – ICANN 2021*, pp. 151–162, Cham, 2021. Springer International Publishing. ISBN 978-3-030-86380-7. doi:[10.1007/978-3-030-86380-7_13](https://doi.org/10.1007/978-3-030-86380-7_13).
- Bungert, L., Raab, R., Roith, T., Schwinn, L., and Tenbrinck, D. CLIP: Cheap Lipschitz training of neural networks. In *International Conference on Scale Space and Variational Methods in Computer Vision*, pp. 307–319. Springer, 2021.
- Béthune, L. *Deep learning with Lipschitz constraints*. Theses, Université de Toulouse, February 2024. Issue: 2024TLSES014.
- Chen, T., Lasserre, J. B., Magron, V., and Pauwels, E. Semi-algebraic Optimization for Lipschitz Constants of ReLU Networks. In Larochelle, H., Ranzato, M., Hadsell, R., Balcan, M. F., and Lin, H. (eds.), *Advances in Neural Information Processing Systems*, volume 33, pp. 19189–19200. Curran Associates, Inc., 2020.
- Cisse, M., Bojanowski, P., Grave, E., Dauphin, Y., and Usunier, N. Parseval Networks: Improving Robustness to Adversarial Examples. In Precup, D. and Teh, Y. W. (eds.), *Proceedings of the 34th International Conference on Machine Learning*, volume 70 of *Proceedings of Machine Learning Research*, pp. 854–863. PMLR, 2017.
- Dubach, R., Abdallah, M. S., and Poggio, T. Multiplicative Regularization Generalizes Better Than Additive Regularization. Article, Center for Brains, Minds and Machines (CBMM), July 2025. Accepted: 2025-07-02T20:03:52Z.
- Entesari, T., Sharifi, S., and Fazlyab, M. ReachLipBnB: A branch-and-bound method for reachability analysis of neural autonomous systems using Lipschitz bounds. In *2023 IEEE International Conference on Robotics and Automation (ICRA)*, pp. 1003–1010, May 2023. doi:[10.1109/ICRA48891.2023.10160732](https://doi.org/10.1109/ICRA48891.2023.10160732).
- Fazlyab, M., Robey, A., Hassani, H., Morari, M., and Pappas, G. Efficient and Accurate Estimation of Lipschitz Constants for Deep Neural Networks. In *Advances in Neural Information Processing Systems*, volume 32. Curran Associates, Inc., 2019.
- Golowich, N., Rakhlin, A., and Shamir, O. Size-Independent Sample Complexity of Neural Networks. In Bubeck, S., Perchet, V., and Rigollet, P. (eds.), *Proceedings of the 31st Conference On Learning Theory*, volume 75 of *Proceedings of Machine Learning Research*, pp. 297–299. PMLR, 2018.
- Gouk, H., Frank, E., Pfahringer, B., and Cree, M. J. Regularisation of neural networks by enforcing Lipschitz continuity. *Machine Learning*, 110(2):393–416, February 2021. ISSN 0885-6125, 1573-0565. doi:[10.1007/s10994-020-05929-w](https://doi.org/10.1007/s10994-020-05929-w).
- He, K., Zhang, X., Ren, S., and Sun, J. Delving Deep into Rectifiers: Surpassing Human-Level Performance on ImageNet Classification. In *2015 IEEE International Conference on Computer Vision (ICCV)*, pp. 1026–1034, December 2015. doi:[10.1109/ICCV.2015.123](https://doi.org/10.1109/ICCV.2015.123). ISSN: 2380-7504.
- Hoffman, J., Roberts, D. A., and Yaida, S. Robust Learning with Jacobian Regularization, August 2019. arXiv:1908.02729 [stat].
- Huang, Y., Zhang, H., Shi, Y., Kolter, J. Z., and Anandkumar, A. Training certifiably robust neural networks with efficient local lipschitz bounds. In *Advances in Neural Information Processing Systems*, volume 34, pp. 22745–22757, 2021.
- Jordan, M. and Dimakis, A. G. Exactly Computing the Local Lipschitz Constant of ReLU Networks. In Larochelle, H., Ranzato, M., Hadsell, R., Balcan, M. F., and Lin, H. (eds.), *Advances in Neural Information Processing Systems*, volume 33, pp. 7344–7353. Curran Associates, Inc., 2020.

- Junnarkar, N., Arcak, M., and Seiler, P. Synthesizing Neural Network Controllers with Closed-Loop Dissipativity Guarantees, April 2024. arXiv:2404.07373 [cs, eess].
- Lai, B.-H., Huang, P.-H., Kung, B.-H., and Chen, S.-T. Enhancing Certified Robustness via Block Reflector Orthogonal Layers and Logit Annealing Loss. In *Forty-second International Conference on Machine Learning*, 2025.
- Lee, S., Lee, J., and Park, S. Lipschitz-certifiable training with a tight outer bound. In *Advances in Neural Information Processing Systems*, volume 33, pp. 16891–16902, 2020.
- Leino, K., Wang, Z., and Fredrikson, M. Globally-robust neural networks. In *International Conference on Machine Learning*, pp. 6212–6222. PMLR, 2021.
- Liu, Z., Wang, Y., Vaidya, S., Ruehle, F., Halverson, J., Soljagic, M., Hou, T. Y., and Tegmark, M. KAN: Kolmogorov–Arnold Networks. In *The Thirteenth International Conference on Learning Representations*, 2025.
- Miyato, T., Kataoka, T., Koyama, M., and Yoshida, Y. Spectral Normalization for Generative Adversarial Networks. In *International Conference on Learning Representations*, 2018.
- Nam, Y., Lee, S. H., Dominé, C. C. J., Park, Y., London, C., Choi, W., Göring, N. A., and Lee, S. Position: Solve Layerwise Linear Models First to Understand Neural Dynamical Phenomena (Neural Collapse, Emergence, Lazy/Rich Regime, and Grokking). June 2025.
- Nenov, R., Haider, D., and Balazs, P. (Almost) Smooth Sailing: Towards Numerical Stability of Neural Networks Through Differentiable Regularization of the Condition Number. In *2nd Differentiable Almost Everything Workshop at the 41st International Conference on Machine Learning*, 2024.
- Neyshabur, B., Salakhutdinov, R. R., and Srebro, N. PathSGD: Path-Normalized Optimization in Deep Neural Networks. In *Advances in Neural Information Processing Systems*, volume 28. Curran Associates, Inc., 2015a.
- Neyshabur, B., Tomioka, R., and Srebro, N. Norm-based capacity control in neural networks. In *Conference on learning theory*, pp. 1376–1401. PMLR, 2015b.
- Neyshabur, B., Tomioka, R., Salakhutdinov, R., and Srebro, N. Data-Dependent Path Normalization in Neural Networks, 2016. eprint: 1511.06747.
- Neyshabur, B., Bhojanapalli, S., and Srebro, N. A PAC-Bayesian Approach to Spectrally-Normalized Margin Bounds for Neural Networks. In *International Conference on Learning Representations*, 2018.
- Orabona, F. and Tommasi, T. Training Deep Networks without Learning Rates Through Coin Betting. In *Advances in Neural Information Processing Systems*, volume 30. Curran Associates, Inc., 2017.
- Pauli, P., Koch, A., Berberich, J., Kohler, P., and Allgöwer, F. Training robust neural networks using Lipschitz bounds. *IEEE Control Systems Letters*, 6:121–126, 2021. Publisher: IEEE.
- Raghunathan, A., Steinhardt, J., and Liang, P. Certified Defenses against Adversarial Examples. February 2018.
- Revay, M., Wang, R., and Manchester, I. R. Recurrent Equilibrium Networks: Flexible Dynamic Models With Guaranteed Stability and Robustness. *IEEE Transactions on Automatic Control*, 69(5):2855–2870, May 2024. ISSN 1558-2523. doi:10.1109/TAC.2023.3294101.
- Sbihi, M., Jan, S., and Couellan, N. MIQCQP reformulation of the ReLU neural networks Lipschitz constant estimation problem, February 2024. arXiv:2402.01199 [math].
- Shang, W., Sohn, K., Almeida, D., and Lee, H. Understanding and improving convolutional neural networks via concatenated rectified linear units. In *international conference on machine learning*, pp. 2217–2225. PMLR, 2016.
- Shi, Z., Wang, Y., Zhang, H., Kolter, J. Z., and Hsieh, C.-J. Efficiently computing local lipschitz constants of neural networks via bound propagation. *Advances in Neural Information Processing Systems*, 35:2350–2364, 2022.
- Shi, Z., Jin, Q., Kolter, Z., Jana, S., Hsieh, C.-J., and Zhang, H. Neural Network Verification with Branch-and-Bound for General Nonlinearities, February 2025. arXiv:2405.21063 [cs].
- Singla, S., Singla, S., and Feizi, S. Improved deterministic l2 robustness on CIFAR-10 and CIFAR-100. In *International Conference on Learning Representations*, 2022.
- Sitzmann, V., Martel, J., Bergman, A., Lindell, D., and Wetzstein, G. Implicit Neural Representations with Periodic Activation Functions. In *Advances in Neural Information Processing Systems*, volume 33, pp. 7462–7473. Curran Associates, Inc., 2020.
- Szegedy, C., Zaremba, W., Sutskever, I., Bruna, J., Erhan, D., Goodfellow, I., and Fergus, R. Intriguing properties of neural networks, February 2014. arXiv:1312.6199 [cs].
- Virmaux, A. and Scaman, K. Lipschitz Regularity of Deep Neural Networks: Analysis and Efficient Estimation. In Bengio, S., Wallach, H., Larochelle, H., Grauman, K., Cesa-Bianchi, N., and Garnett, R. (eds.), *Advances in*

- Neural Information Processing Systems*, volume 31. Curran Associates, Inc., 2018.
- Wainwright, M. J. *High-Dimensional Statistics: A Non-Asymptotic Viewpoint*. Cambridge Series in Statistical and Probabilistic Mathematics. Cambridge University Press, Cambridge, 2019. ISBN 978-1-108-49802-9. doi:10.1017/9781108627771.
- Wang, R. and Manchester, I. Direct parameterization of lipschitz-bounded deep networks. In *International Conference on Machine Learning*, pp. 36093–36110. PMLR, 2023.
- Weng, L., Zhang, H., Chen, H., Song, Z., Hsieh, C.-J., Daniel, L., Boning, D., and Dhillon, I. Towards fast computation of certified robustness for relu networks. In *International Conference on Machine Learning*, pp. 5276–5285. PMLR, 2018.
- Wong, E. and Kolter, Z. Provable defenses against adversarial examples via the convex outer adversarial polytope. In *International conference on machine learning*, pp. 5286–5295. PMLR, 2018.
- Xu, Y. and Sivaranjani, S. Learning Dissipative Neural Dynamical Systems. *IEEE Control Systems Letters*, 7:3531–3536, 2023. ISSN 2475-1456. doi:10.1109/LCSYS.2023.3337851.
- Xu, Y. and Sivaranjani, S. ECLipsE: Efficient Compositional Lipschitz Constant Estimation for Deep Neural Networks. In Globerson, A., Mackey, L., Belgrave, D., Fan, A., Paquet, U., Tomczak, J., and Zhang, C. (eds.), *Advances in Neural Information Processing Systems*, volume 37, pp. 10414–10441. Curran Associates, Inc., 2024.
- Xu, Y. and Sivaranjani, S. ECLipsE-Gen-Local: Efficient Compositional Local Lipschitz Estimates for Deep Neural Networks, October 2025. arXiv:2510.05261 [cs].
- Yoshida, Y. and Miyato, T. Spectral Norm Regularization for Improving the Generalizability of Deep Learning, May 2017. arXiv:1705.10941 [stat].
- Zhang, H., Weng, T.-W., Chen, P.-Y., Hsieh, C.-J., and Daniel, L. Efficient neural network robustness certification with general activation functions. *Advances in neural information processing systems*, 31, 2018.
- Zhang, H., Zhang, P., and Hsieh, C.-J. RecurJac: An Efficient Recursive Algorithm for Bounding Jacobian Matrix of Neural Networks and Its Applications. *Proceedings of the AAAI Conference on Artificial Intelligence*, 33(01): 5757–5764, July 2019. ISSN 2374-3468, 2159-5399. doi:10.1609/aaai.v33i01.33015757.

Contents

1	Introduction	1
2	Preliminaries	3
3	Mitigating weaknesses of the trivial bound	3
3.1	Dead neurons	3
3.1.1	Polyactivations	3
3.2	Biases	4
3.2.1	Rectangular sinusoidal layers	4
3.3	Ill-conditioned weight matrices	5
3.3.1	Lipschitz penalty	5
4	Theoretical and practical lower bounds	6
4.1	An empirical bound	6
5	Experimental results	6
5.1	Iris dataset: upper and lower 2-norm Lipschitz bounds on a shallow network	7
5.2	MNIST dataset: Lipschitz bounds	7
6	Conclusion	8
A	Objections to the trivial bound considered	14
B	Supplement to Section 3	15
C	Supplement to Section 5	20
C.1	Iris: methodology	20
C.2	Iris: results	20
C.3	MNIST: methodology	23
C.4	MNIST: results	23
D	Additional experiments on MNIST	24
D.1	Other (poly-)activations	24
D.2	Regularization in $p = 1$ and $p = \infty$	25
D.3	Other penalties	29
D.4	Comparison to a direct parameterization	32

List of Figures

5.1	MNIST experiment: normalized singular values of the weight matrices (with and without penalty).	7
-----	---	---

C.1	Iris experiment: training curves for $\lambda = 0$ (left) and $\lambda = 10^{-2}$ (right). Shaded area indicates the gap between theoretical upper and lower bounds on the Lipschitz constant.	20
C.2	Iris experiment: decision boundaries in 2D principal component planes for $\lambda = 0$. (Training data)	21
C.3	Iris experiment: decision boundaries in 2D principal component planes for $\lambda = 10^{-2}$. (Training data)	22
C.4	MNIST experiment: PGD attack success rate (with and without penalty).	23
C.5	MNIST experiment: training curves (with and without penalty).	24
D.1	MNIST experiment: normalized row norms of weight matrices for $p = \infty$ norm (with and without penalty).	27
D.2	MNIST experiment: normalized column norms of weight matrices for $p = 1$ norm (with and without penalty).	27
D.3	MNIST experiment: normalized singular values of the weight matrices for alternative regularization methods.	29
D.4	MNIST experiment: PGD attack error rates for alternative regularization methods.	30
D.5	MNIST experiment: training curves for alternative regularization methods.	31
D.6	MNIST experiment: PGD attack error rates for direct parameterization comparison.	32
D.7	MNIST experiment: training curves for direct parameterization comparison.	33

List of Tables

5.1	Iris experiment: final predictive performance after 20,000 steps.	7
5.2	Iris experiment: 2-norm Lipschitz upper bound K versus lower bounds. Here $K/(\sqrt{2}\kappa(W))$ is the guaranteed lower bound from Theorem 4.1, while \widehat{L} is an empirical lower bound from local optimization of the Lipschitz ratio over input pairs.	7
5.3	MNIST experiment: 2-norm Lipschitz upper bound K versus empirical lower bound \widehat{L}	8
C.1	MNIST experiment: PGD attack error rates (%) at various perturbation radii ϵ	23
D.1	MNIST experiment: PGD attack error rates (%) for various activations with Lipschitz regularization ($\lambda = 10^{-2}$). emp = empirical, cert = certified.	25
D.2	MNIST experiment: Lipschitz bounds and predictive performance for various activations with Lipschitz regularization ($\lambda = 10^{-2}$).	25
D.3	MNIST experiment: Lipschitz bounds for $p = \infty$ norm with various activations.	26
D.4	MNIST experiment: Predictive performance for $p = \infty$ norm with various activations.	26
D.5	MNIST experiment: Lipschitz bounds for $p = 1$ norm with various activations.	26
D.6	MNIST experiment: Predictive performance for $p = 1$ norm with various activations.	28
D.7	MNIST experiment: PGD attack error rates (%) for $p = \infty$ norm with various activations. emp = empirical, cert = certified.	28
D.8	MNIST experiment: PGD attack error rates (%) for $p = 1$ norm with various activations. emp = empirical, cert = certified.	28
D.9	MNIST experiment: PGD attack error rates (%) for alternative regularization methods.	30
D.10	MNIST experiment: Comparison of alternative regularization methods.	30
D.11	MNIST experiment: Predictive performance for direct parameterization comparison.	33
D.12	MNIST experiment: PGD attack error rates (%) for direct parameterization comparison.	33

A. Objections to the trivial bound considered

Aiming at the broader objective of Lipschitz and robust training and verification, and having argued for the uncommon⁵ path of least resistance—penalizing the product of induced matrix norms—over more sophisticated methods, we are therefore behooved to address its discontents in kind.

Trivial bound too loose Some argue that the trivial Lipschitz bound should not be penalized directly: because the trivial Lipschitz bound is known to be loose in deeper networks, penalizing it is an overly restrictive regularization. For this reason, it is better to enforce a semidefinite constraint (a tighter Lipschitz bound) on the matrix weights (Raghunathan et al., 2018; Wang & Manchester, 2023; Xu & Sivaranjani, 2023; Revay et al., 2024; Junnarkar et al., 2024).

We reply that, as the example in §3.3 shows for the toy problem of learning a linear function, the looseness of the trivial Lipschitz bound can be optimized away. Our experiments support a similar claim for nonlinear networks, and Figure 5.1 shows that the same mechanism is at play.

Qualitatively, the induced norm is a slacker penalty than Tikhonov regularization such as weight decay, which penalizes the Frobenius norm. For $p = 2$, the induced norm penalty is only active on the largest singular value of each weight matrix and has a rank-1 gradient, while the Frobenius norm penalty is active on all singular values (leading to a full-rank gradient). Just like ∞ -norm regularization tends to lead to anti-sparse vectors in convex problems, the spectral norm penalty leads to well-conditioned weight matrices because optimizing the lower singular spaces is “free.”

Lipschitz-constrained parameterization The trivial Lipschitz bound is less conservative when weight matrices are well-conditioned. Therefore, it is better to constrain the weight matrices to be well-conditioned and Lipschitz by parameterization, either by projected gradient descent onto layerwise Lipschitz balls (Gouk et al., 2021) or by direct parameterization of the Lipschitz cylinder (Cisse et al., 2017; Singla et al., 2022; Wang & Manchester, 2023; Lai et al., 2025; Béthune, 2024).

We reply that parameterizations such as the exponential map onto the Stiefel manifold are computationally expensive and strongly curved, leading to challenges in training. This is a motivation for Wang & Manchester (2023), which uses a matrix factorization to parameterize weight matrices that satisfy a semidefinite constraint for the ReLU activation. However, the ReLU activation is intrinsically Lipschitz-inefficient (Section 3.1), and the technology of semidefinite programming is more complicated than multiplicative trivial bounds.

Moreover, despite the connection via Lagrange multipliers, a Lipschitz constraint may prove more statistically fragile than Lipschitz regularization. This conjecture is supported by an analogy to the Lasso, which is more robust to its hyperparameter in penalty form than in its constrained or basis pursuit forms (Wainwright, 2019, Chapter 7).

Alternatively, well-conditioned weight matrices may be achieved by penalizing the sum of the quantities $\frac{1}{2} \|W\|_2^2 - \frac{1}{2n} \|W\|_F^2$ for each weight matrix W (Nenov et al., 2024). We reply that well-conditioning is necessary but not sufficient for a tight trivial Lipschitz bound. The $\frac{1}{2} \|W\|_F^2$ term in the ill-conditioning loss is strictly more complicated and not directly related to the ultimate goal of minimizing the Lipschitz constant.

Numerical considerations Some have reported that it is hard to train networks with a Lipschitz penalty, because “the product of norms can be very large” (Gouk et al., 2021). It is therefore better to penalize the average of the induced matrix norms, which is additionally convex (Yoshida & Miyato, 2017).

We answer, first, that floating-point precision has more than enough headroom to handle the product of induced norms. Modern optimizers such as the “Ada-” family and Cocob (Orabona & Tommasi, 2017) with gradient-norm adaptation can handle the initially large gradient of the product of induced norms and its decay by several orders of magnitude over later optimization steps.

We answer, second, that penalizing the average of induced norms is not directly related to the ultimate goal of minimizing the Lipschitz constant. Concavity is the point: to minimize a product of nonnegative numbers, one focuses on the smallest term. By the AM-GM inequality, the product of induced norms is a *less* onerous penalty than the sum of the induced norms.

Computational complexity Minimizing the product of induced matrix norms is computationally intractable in the case of $p = 2$, because the spectral norms and their gradients are expensive to compute, necessitating the use of e.g. power iteration

⁵The closest idea is Dubach et al. (2025), which penalizes the product of Frobenius norms.

(Yoshida & Miyato, 2017; Miyato et al., 2018).

We find that computing the eigenvector corresponding to the largest eigenvalue of WW^\top is fast enough to run inside a minibatch loop. If training time is a priority, we may instead target the Lipschitz constant in $p = 1$ or, as in Raghunathan et al. (2018), $p = \infty$, using a p -saturating polyactivation proposed in §3.1.1. This would sacrifice the bias-robust property of cos/sin activation (which saturate the 2-norm), but comes with the advantage that the $p \in \{1, \infty\}$ induced norms are fast to compute and differentiate.

B. Supplement to Section 3

Proof of Theorem 3.3 (ASL). The Jacobian of the ASL unit $x \mapsto \sigma(Wx + b)$ is

$$x \mapsto \text{diag}(\sigma'(Wx + b)) W.$$

Suppose that σ achieves its steepest slope at z_0 . For generic W and b , there exists a preimage x_0 such that $Wx_0 + b = z_0\mathbf{1}$. At $x = x_0$, $\text{diag}(\sigma'(Wx + b))$ becomes the scalar matrix $\sigma'(z_0)I$, and the Jacobian equals $\sigma'(z_0)W$. The trivial Lipschitz bound is tight by the homogeneity of induced matrix norm. \square

Proof of Theorem 3.3 (SLA). The Jacobian of the SLA unit $x \mapsto W\sigma(x) + b$ is

$$x \mapsto W \text{diag}(\sigma'(x)),$$

which achieves the trivial Lipschitz bound in the p -norm at $x = z_0\mathbf{1}$. \square

Proof of Theorem 3.3 (LAS). The Jacobian of the LAS unit $x \mapsto W\sigma(x + b)$ is

$$x \mapsto W \text{diag}(\sigma'(x + b)),$$

which achieves the trivial Lipschitz bound in the p -norm at $x = z_0\mathbf{1} - b$. \square

Proof of Theorem 3.4 (ReLU). Consider the neural network $\mathbb{R} \rightarrow \mathbb{R}$ defined by

$$x \mapsto \sum_{i=1}^d (-1)^i \text{ReLU}(x + b_i) = W^1 \text{ReLU}(W^0 x + b)$$

where

$$\begin{aligned} W^1 &= (-1, 1, -1, \dots)^\top \\ W^0 &= (1, 1, 1, \dots) \\ b &= (1, 2, 3, \dots) \end{aligned}$$

The true Lipschitz constant is 1, but the trivial 2-Lipschitz bound is

$$\underbrace{\|W^1\|_2}_{=\sqrt{d}} \underbrace{\|W^0\|_2}_{=\sqrt{d}} = d.$$

On the other hand, if the bias is changed to

$$b' = (1, -1, 1, -1, \dots),$$

then the true Lipschitz constant is $\Omega(d)$. \square

Proof of Theorem 3.4 (tanh). The idea is to toggle between overlapping and non-overlapping regions of the hyperbolic tangent function. Consider the neural network $\mathbb{R} \rightarrow \mathbb{R}$ defined by

$$x \mapsto \sum_{i=1}^d \tanh(x + b_i) = \mathbf{1}^\top \tanh(\mathbf{1}x + b).$$

The trivial 2-Lipschitz bound is $\Omega(d)$ and is achieved by $b = 0$. But if the biases are changed to

$$b' = (1, 2, 3, \dots),$$

then the true Lipschitz constant is

$$\sup_x \sum_{i=1}^d \operatorname{sech}^2(x + i) = O(1).$$

□

Proof of Theorem 3.5. Consider the LASL unit $f_b : \mathbb{R} \rightarrow \mathbb{R}$ defined by

$$f_b(x) = \mathbf{1}^\top \sin(\mathbf{1}x + b) = \sum_{i=1}^{2d} \sin(x + b_i),$$

where $\mathbf{1} \in \mathbb{R}^{2d}$ is the vector of ones and $b \in \mathbb{R}^{2d}$ is a bias vector. The trivial 2-Lipschitz bound equals

$$\|\mathbf{1}^\top\|_2 \|\mathbf{1}\|_2 = \|\mathbf{1}\|_2^2 = 2d = \Omega(d),$$

since $|\sin'(\cdot)| \leq 1$.

On one hand, if we take $b = 0$, the true Lipschitz constant is $2d$, and the trivial bound is tight.

On the other hand, if we take $b_i = i\pi$ for all i , then each sine term cancels out with its neighbor, resulting in a constant function with Lipschitz constant 0. □

Proof of Theorem 3.8. 1 \iff 2 follows from the fact that $K = 1$ is achievable, and K cannot be less than 1:

$$\begin{aligned} 1 = \|I\| &= \|W_L W_{L-1} \cdots W_1\| \\ &\leq \|W_L\| \|W_{L-1}\| \cdots \|W_1\| = K. \end{aligned}$$

2 \implies 3 by the calculation

$$\begin{aligned} 1 = K &\geq \|W_L\| \|W_{L-1} \cdots W_1\| \\ &= \|W_L\| \|W_L^{-1}\| = \kappa(W_L) \end{aligned}$$

and induction on L .

3 \implies 1 by the fact that each $W_i, i \in \{1, \dots, L\}$, is a scalar multiple of an orthogonal matrix, and the product of orthogonal matrices is orthogonal. □

Proof of Theorem 4.1. The Jacobian of f is

$$Df(x) = \begin{pmatrix} -A & B \end{pmatrix} \begin{pmatrix} \operatorname{Sin}(Wx) \\ \operatorname{Cos}(Wx) \end{pmatrix} W.$$

We use the probabilistic method to argue for the existence of an $x^* \in \mathbb{R}^r$ such that $\|Df(x^*)\|_2$ is large. Assign a probability measure to X such that $Y = WX$ has the uniform distribution on the torus $[-\pi, \pi]^n$. Define

$$\Sigma^* = \mathbb{E} Df(X) Df(X)^\top = \begin{pmatrix} -A & B \end{pmatrix} Q \begin{pmatrix} -A^\top \\ B^\top \end{pmatrix},$$

where

$$Q = \begin{bmatrix} \operatorname{Sin}(Y) W W^\top \operatorname{Sin}(Y) & \operatorname{Sin}(Y) W W^\top \operatorname{Cos}(Y) \\ \operatorname{Cos}(Y) W W^\top \operatorname{Sin}(Y) & \operatorname{Cos}(Y) W W^\top \operatorname{Cos}(Y) \end{bmatrix}.$$

Taking expectations, we get

$$\mathbb{E} Q = \frac{1}{2} \begin{pmatrix} \text{Diag}(WW^\top) & 0 \\ 0 & \text{Diag}(WW^\top) \end{pmatrix} \quad (6)$$

which implies that

$$\mathbb{E} Df(X)Df(X)^\top \geq \frac{1}{2} (A \text{Diag}(WW^\top) A^\top + B \text{Diag}(WW^\top) B^\top).$$

Because λ_{\max} is convex,

$$\mathbb{E} \lambda_{\max}(Df(X)Df(X)^\top) \geq \frac{1}{2} \lambda_{\max}(A \text{Diag}(WW^\top) A^\top + B \text{Diag}(WW^\top) B^\top).$$

Therefore there exists an x^* such that

$$\|Df(x^*)\|_2^2 \geq \frac{1}{2} \lambda_{\max}(A \text{Diag}(WW^\top) A^\top + B \text{Diag}(WW^\top) B^\top).$$

To get a closed form, use the fact that

$$\text{Diag}(WW^\top) \geq \lambda_{\min}(WW^\top)I.$$

□

Theorem B.1 (Lower bound on absolute value networks). *Let $f(x)$ be an LASL unit from $\mathbb{R}^n \rightarrow \mathbb{R}^n \rightarrow \mathbb{R}^m$ given by Equation (2),*

$$f(x) = A \text{abs}(Wx).$$

Then, if W has full rank, the following Lipschitz lower bound holds:

$$\|f\|_{\text{Lip},2}^2 \geq \frac{1}{2} \lambda_{\max}(A \text{Diag}(WW^\top) A^\top),$$

and the trivial Lipschitz bound

$$K = \|A\|_2 \|W\|_2$$

is off by less than a factor of $\kappa(W)$:

$$\frac{1}{\kappa(W)} K \leq \|f\|_{\text{Lip},2} \leq K,$$

where $\kappa(W) = \sqrt{\lambda_{\max}(WW^\top)/\lambda_{\min}(WW^\top)}$ is the condition number.

Proof of Theorem B.1. The Jacobian of f is

$$Df(x) = A \text{diag}(\text{sgn}(Wx)) W,$$

where sgn is the sign function. We use the probabilistic method to argue for the existence of an $x^* \in \mathbb{R}^n$ such that $\|Df(x^*)\|_2$ is large. Assign a probability measure to X such that $S = \text{sgn}(WX)$ has the Rademacher distribution, i.e., each component is independently ± 1 with equal probability. Define

$$\begin{aligned} \Sigma^* &= \mathbb{E} Df(X)Df(X)^\top \\ &= A \mathbb{E} (\text{Diag}(S)WW^\top \text{Diag}(S)) A^\top. \end{aligned}$$

Taking expectations, we get

$$\mathbb{E} (\text{Diag}(S)WW^\top \text{Diag}(S)) = \text{Diag}(WW^\top),$$

which implies that

$$\mathbb{E} Df(X)Df(X)^\top = A \text{Diag}(WW^\top) A^\top.$$

Because λ_{\max} is convex,

$$\mathbb{E} \lambda_{\max}(Df(X)Df(X)^\top) \geq \lambda_{\max}(A \text{Diag}(WW^\top) A^\top).$$

Therefore there exists an x^* such that

$$\|Df(x^*)\|_2^2 \geq \lambda_{\max}(A \text{Diag}(WW^\top) A^\top).$$

□

Theorem B.2. Let $f : \mathbb{R}^{d_0} \rightarrow \mathbb{R}^{d_L}$ be a depth- L network defined by

$$\begin{aligned} f(x) &= z^L, \\ z^\ell &= A^\ell \cos(z^{\ell-1}) + B^\ell \sin(z^{\ell-1}), & \ell = 1, \dots, L, \\ z^0 &= x. \end{aligned}$$

Fix a scale $\alpha > 0$. Initialize each pair (A^ℓ, B^ℓ) from the random-phase initialization Equation (5) at scale α . Then for every $x \in \mathbb{R}^{d_0}$,

$$\mathbb{E}(Df(x)Df(x)^\top) = \alpha^L I.$$

Proof. By trigonometric identities, this network is equivalent to

$$\begin{aligned} f(x) &= z^L, \\ z^\ell &= \bar{A}^\ell \cos(z^{\ell-1} + \theta^\ell) + \bar{B}^\ell \sin(z^{\ell-1} + \theta^\ell), \\ z^0 &= x. \end{aligned}$$

Taking derivatives with respect to x , we get

$$\begin{aligned} D_x f(x) &= D_x z^L, \\ D_x z^\ell &= \begin{pmatrix} -\bar{A}^\ell & \bar{B}^\ell \end{pmatrix} \begin{pmatrix} \text{Sin}(z^{\ell-1} + \theta^\ell) \\ \text{Cos}(z^{\ell-1} + \theta^\ell) \end{pmatrix} D_x z^{\ell-1}, \\ D_x z^0 &= I. \end{aligned}$$

Write $Q^\ell = D_x z^\ell (D_x z^\ell)^\top$. Then we are interested in $\mathbb{E} Q^L$, where

$$Q^\ell = \begin{pmatrix} -\bar{A}^\ell & \bar{B}^\ell \end{pmatrix} \begin{pmatrix} \text{Sin}(z^{\ell-1} + \theta^\ell) \\ \text{Cos}(z^{\ell-1} + \theta^\ell) \end{pmatrix} Q^{\ell-1} \begin{pmatrix} \text{Sin}(z^{\ell-1} + \theta^\ell) \\ \text{Cos}(z^{\ell-1} + \theta^\ell) \end{pmatrix}^\top \begin{pmatrix} -\bar{A}^\ell & \bar{B}^\ell \end{pmatrix}^\top$$

and $Q^0 = I$. Using the fact that $z^{\ell-1} + \theta^\ell$ is independent and uniformly distributed on the unit circle $\mathbb{R}/2\pi\mathbb{Z}$ irrespective of the (unknown) distribution of $z^{\ell-1}$, we take the expectation of the inner three matrices to get

$$\mathbb{E}(Q^\ell | A^\ell, B^\ell) = \frac{1}{2} \begin{pmatrix} -\bar{A}^\ell & \bar{B}^\ell \end{pmatrix} \mathbb{E} Q^{\ell-1} \begin{pmatrix} -(\bar{A}^\ell)^\top \\ (\bar{B}^\ell)^\top \end{pmatrix}.$$

Now we will prove by induction on ℓ that $\mathbb{E} Q^\ell = \alpha^\ell I$. The case $\ell = 0$ is clear. Assume the claim holds for $\ell - 1$. We know *a fortiori* that $\mathbb{E} Q^{\ell-1}$ is a scalar matrix and commutes with matrix multiplication, leading to

$$\begin{aligned} \mathbb{E}(Q^\ell | A^\ell, B^\ell) &= \alpha^{\ell-1} \frac{1}{2} \begin{pmatrix} -\bar{A}^\ell & \bar{B}^\ell \end{pmatrix} \begin{pmatrix} -(\bar{A}^\ell)^\top \\ (\bar{B}^\ell)^\top \end{pmatrix} \\ &= \alpha^{\ell-1} \frac{1}{2} \left(\bar{A}^\ell (\bar{A}^\ell)^\top + \bar{B}^\ell (\bar{B}^\ell)^\top \right) \end{aligned}$$

Using the Law of Total Expectation and the fact that

$$\mathbb{E} \bar{A}^\ell (\bar{A}^\ell)^\top = \mathbb{E} \bar{B}^\ell (\bar{B}^\ell)^\top = \alpha I,$$

we get

$$\mathbb{E} Q^\ell = \alpha^\ell I.$$

□

C. Supplement to Section 5

We implement neural networks using Equinox and train them using the Cocob optimizer, provided in Optax. The datasets are Iris, provided by SciKit-learn, and MNIST, provided by HuggingFace datasets.

C.1. Iris: methodology

We train a small classifier on the Iris dataset (4 features, 3 classes) with standardized inputs and a stratified 80/20 train/test split (120/30). The model is a 2-layer MLP with one hidden layer of width 4 and the (\cos, \sin) polyactivation (implemented as `SinCosTwo`). Up to an additive bias (which does not affect Lipschitz constants), the network can be written in the LASL form of Equation (2), $f(x) = A \cos(Wx) + B \sin(Wx)$, so that the standard product-of-layer 2-norm bound equals the trivial LASL bound in Theorem 4.1,

$$K = \left\| \begin{pmatrix} A & B \end{pmatrix} \right\|_2 \|W\|_2.$$

Optimization consisted of full-batch Cocob for 20,000 steps.

C.2. Iris: results

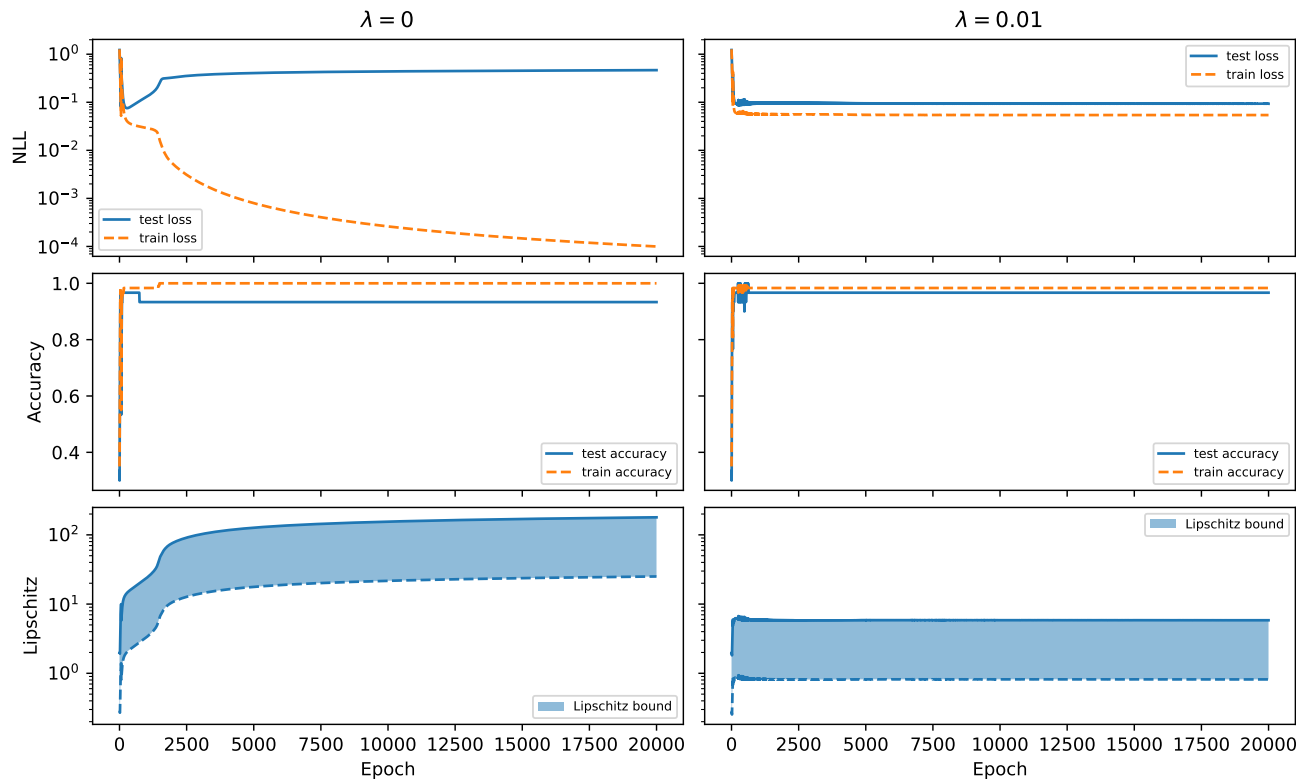


Figure C.1. Iris experiment: training curves for $\lambda = 0$ (left) and $\lambda = 10^{-2}$ (right). Shaded area indicates the gap between theoretical upper and lower bounds on the Lipschitz constant.

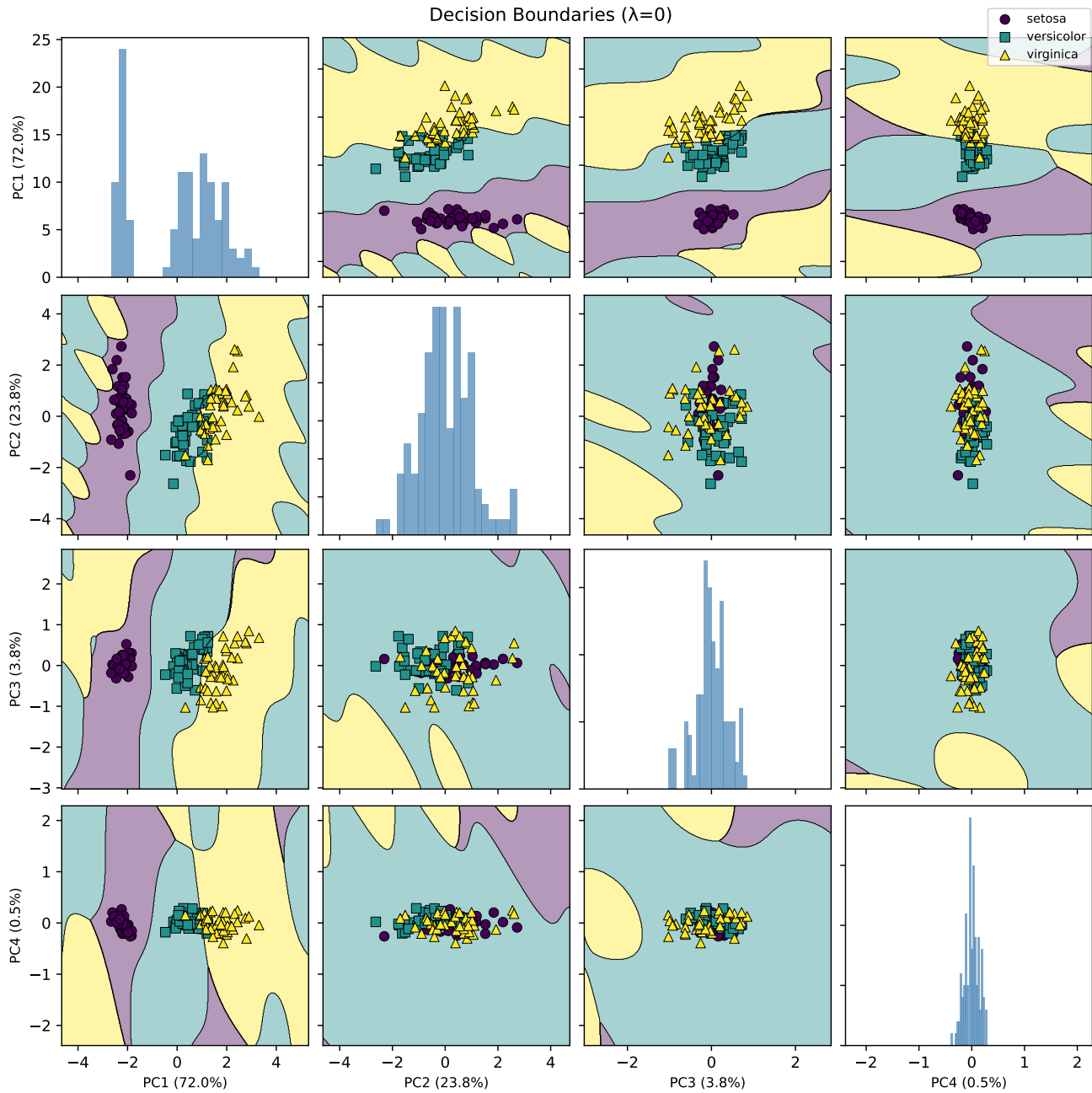


Figure C.2. Iris experiment: decision boundaries in 2D principal component planes for $\lambda = 0$. (Training data)

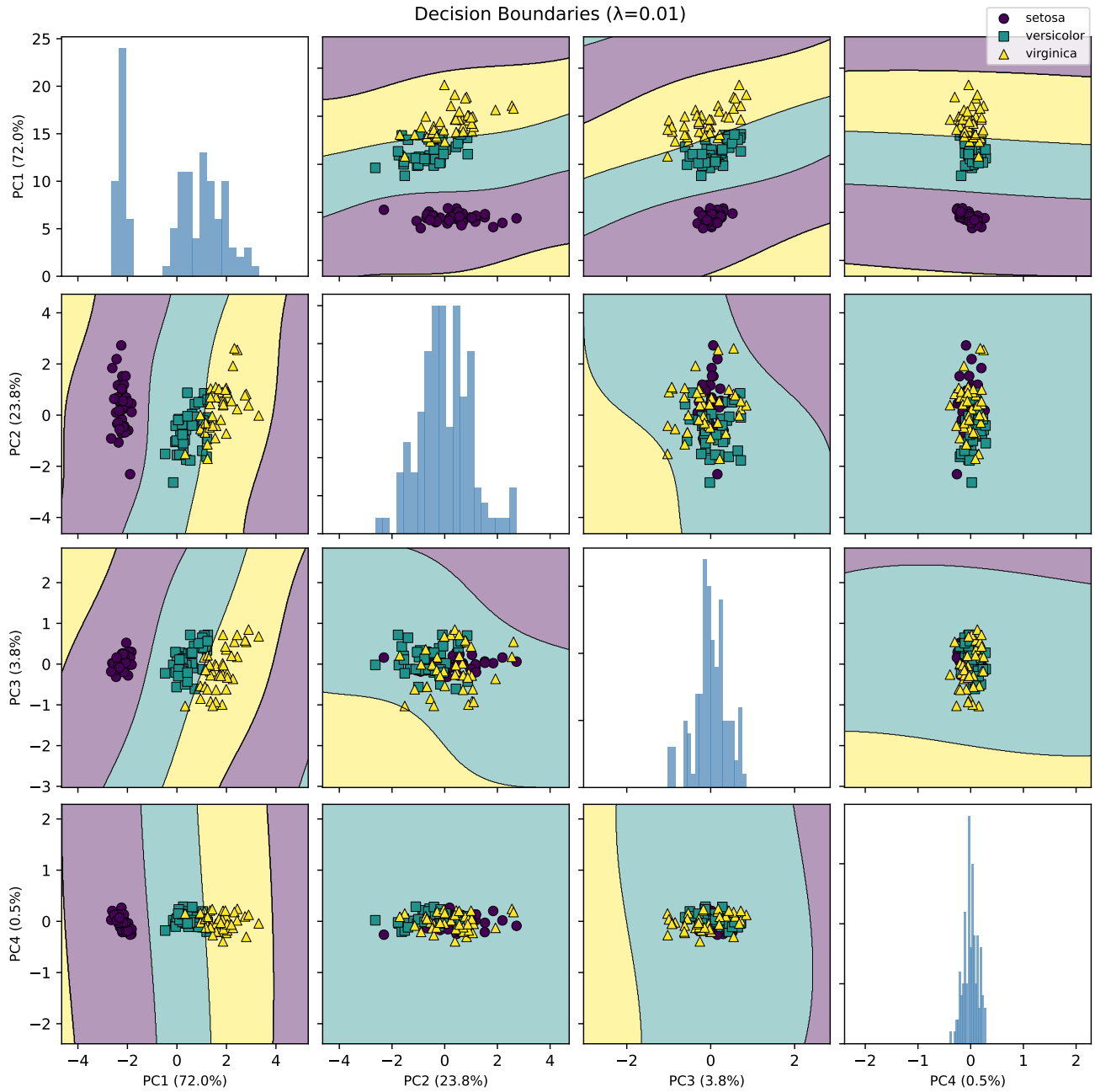


Figure C.3. Iris experiment: decision boundaries in 2D principal component planes for $\lambda = 10^{-2}$. (Training data)

C.3. MNIST: methodology

We train a classifier on MNIST to assess our 2-norm Lipschitz training proposal on a larger model. The network takes normalized 28×28 images flattened into \mathbb{R}^{784} and uses two hidden layers of width 128 with the 2-norm saturated polyactivation (\cos, \sin). For each choice of regularization weight $\lambda \in \{0, 10^{-2}\}$, we minimize the cross-entropy loss augmented with a penalty on the global 2-norm Lipschitz upper bound K , computed as the product of per-layer spectral-norm bounds. We use a uniform-phase stable initialization (Thm. B.2, $\alpha = 2^{-1/2}$) for the weights and train for 80 epochs with batch size 60 using the parameter-free Cocob optimizer. We report standard deviation over the ensemble of random initializations.

C.4. MNIST: results

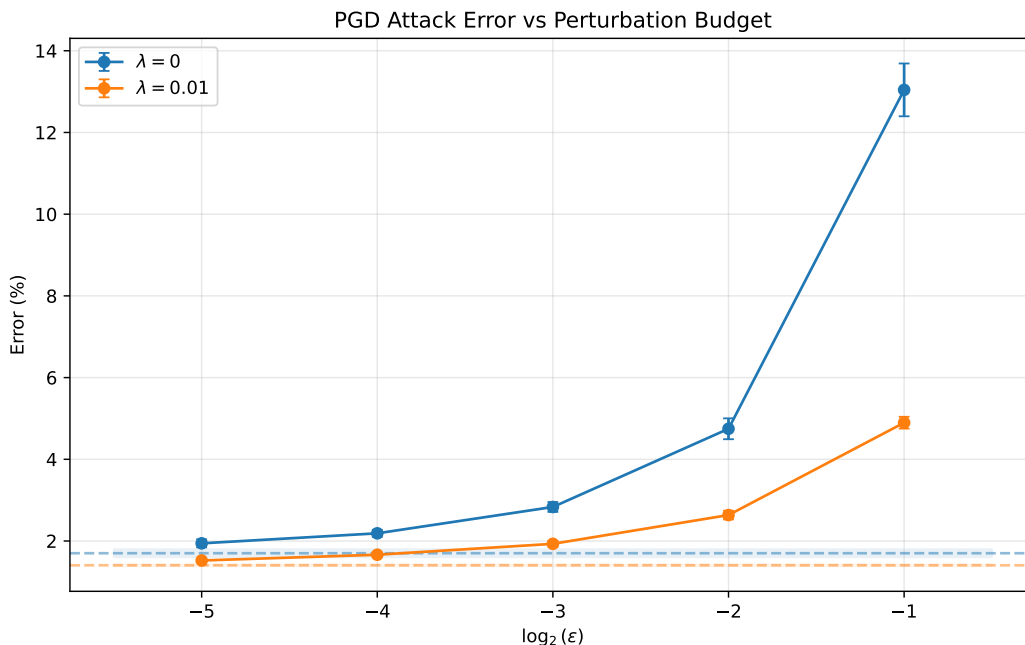


Figure C.4. MNIST experiment: PGD attack success rate (with and without penalty).

Table C.1. MNIST experiment: PGD attack error rates (%) at various perturbation radii ϵ .

λ		Clean	$\epsilon = 2^{-1}$	$\epsilon = 2^{-2}$	$\epsilon = 2^{-3}$	$\epsilon = 2^{-4}$	$\epsilon = 2^{-5}$
0	empirical	1.70 ± 0.10	13.04 ± 0.65	4.75 ± 0.26	2.83 ± 0.12	2.19 ± 0.09	1.94 ± 0.10
	certified		100.00 ± 0.00	100.00 ± 0.00	100.00 ± 0.00	89.99 ± 9.61	14.47 ± 4.01
10^{-2}	empirical	1.41 ± 0.02	4.90 ± 0.14	2.64 ± 0.11	1.93 ± 0.07	1.66 ± 0.05	1.52 ± 0.03
	certified		31.60 ± 0.66	7.66 ± 0.23	3.34 ± 0.12	2.15 ± 0.09	1.76 ± 0.06

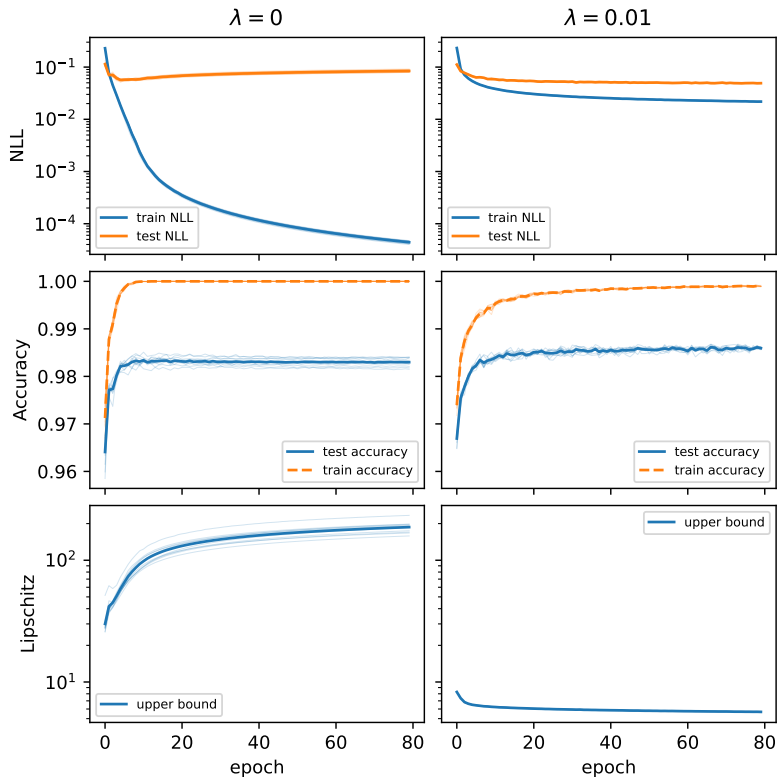


Figure C.5. MNIST experiment: training curves (with and without penalty).

D. Additional experiments on MNIST

D.1. Other (poly-)activations

Is a tightly trained Lipschitz constant compelling enough to displace popular activations such as ReLU and tanh? The advantages of (cos, sin) polyactivation are:

- It is closed under input translations, so each hidden layer is a universal approximant.
- It doubles the number of parameters per layer, allowing more degrees of freedom to economize the trivial Lipschitz bound without impacting performance.
- It saturates the 2-norm, maximally utilizing “Lipschitz capacity” (Anil et al., 2019).

What does Lipschitz regularization have to offer when these properties are relaxed?

Methodology We repeat the MNIST experiment Section 5.2 with a third order tanh polyactivation (Example 3), CReLU, abs, and ReLU (which is not saturated) to illustrate the relative effect of each property.

Results From the PGD success rates (Table D.1) and the Lipschitz bounds and predictive performance (Table D.2), we find that ReLU has the highest Lipschitz upper and lower bounds, which correlates with the highest PGD success rates. This supports our claim that ReLU is not suited for the trivial Lipschitz bound.

Table D.1. MNIST experiment: PGD attack error rates (%) for various activations with Lipschitz regularization ($\lambda = 10^{-2}$). emp = empirical, cert = certified.

Polyactivation		$\epsilon = 2^{-1}$	$\epsilon = 2^{-2}$	$\epsilon = 2^{-3}$	$\epsilon = 2^{-4}$	$\epsilon = 2^{-5}$
(cos, sin)	emp	4.90 ± 0.18	2.54 ± 0.09	1.91 ± 0.04	1.64 ± 0.05	1.50 ± 0.05
	cert	31.31 ± 0.59	7.58 ± 0.31	3.22 ± 0.09	2.14 ± 0.06	1.73 ± 0.05
(tanh, sech, log cosh)	emp	4.44 ± 0.12	2.38 ± 0.02	1.73 ± 0.11	1.49 ± 0.08	1.37 ± 0.07
	cert	22.98 ± 0.32	6.15 ± 0.15	2.88 ± 0.03	1.91 ± 0.11	1.55 ± 0.07
CReLU	emp	5.44 ± 0.06	2.79 ± 0.07	2.07 ± 0.08	1.79 ± 0.04	1.64 ± 0.04
	cert	28.18 ± 0.40	7.37 ± 0.06	3.28 ± 0.12	2.24 ± 0.08	1.86 ± 0.04
absolute value	emp	7.15 ± 0.14	3.39 ± 0.11	2.37 ± 0.04	2.00 ± 0.04	1.83 ± 0.05
	cert	21.81 ± 0.32	6.60 ± 0.15	3.26 ± 0.15	2.32 ± 0.05	1.98 ± 0.04
ReLU	emp	7.96 ± 0.09	3.82 ± 0.07	2.53 ± 0.06	2.12 ± 0.09	1.93 ± 0.06
	cert	46.05 ± 0.56	11.21 ± 0.11	4.63 ± 0.09	2.86 ± 0.10	2.21 ± 0.06

Table D.2. MNIST experiment: Lipschitz bounds and predictive performance for various activations with Lipschitz regularization ($\lambda = 10^{-2}$).

Polyactivation	K (upper)	\hat{L} (lower)	K/\hat{L}	Train NLL	Test NLL	Test Acc.
(cos, sin)	5.66 ± 0.03	5.15 ± 0.05	1.10	0.0208 ± 0.0003	0.0489 ± 0.0008	98.60 ± 0.04%
(tanh, sech, log cosh)	5.24 ± 0.01	4.78 ± 0.04	1.10	0.0180 ± 0.0002	0.0443 ± 0.0006	98.73 ± 0.05%
CReLU	5.49 ± 0.02	4.60 ± 0.06	1.19	0.0203 ± 0.0001	0.0501 ± 0.0004	98.51 ± 0.04%
absolute value	5.00 ± 0.03	4.91 ± 0.02	1.02	0.0173 ± 0.0003	0.0546 ± 0.0018	98.34 ± 0.08%
ReLU	6.37 ± 0.02	5.88 ± 0.02	1.08	0.0284 ± 0.0002	0.0625 ± 0.0006	98.25 ± 0.07%

D.2. Regularization in $p = 1$ and $p = \infty$

While greater attention has been paid to the operator 2-norm, the basic idea of this paper—directly penalizing the product of induced norms, with a p -saturating polyactivation function—is immediately applicable to the induced 1-norm (maximum absolute column sum) and $p = \infty$ (maximum absolute row sum). Moreover, these induced norms are appealing by virtue of the fact that they scale linearly with the number of parameters. For an $m \times n$ matrix, computing the induced 1-norm or ∞ -norm requires $O(mn)$ operations, whereas computing the induced 2-norm requires $O(\min(m, n) \cdot mn)$ operations via SVD. In our experiments the 1- and ∞ -norm Lipschitz-penalized loss gradients are 4-5x faster to compute than the 2-norm Lipschitz-penalized loss gradient.

Methodology We repeat Section 5.2 using the cross-entropy loss with various 1- and ∞ -norm saturated polyactivations, while penalizing the scaled trivial bounds

$$\frac{\lambda}{\sqrt{\text{num outputs}}} \prod_{\ell=1}^L \|\mathbf{W}_\ell\|_1$$

and

$$\frac{\lambda}{\sqrt{\text{num inputs}}} \prod_{\ell=1}^L \|\mathbf{W}_\ell\|_\infty$$

respectively.

Results We observe that by the end of training, ∞ -norm (Table D.3) and 1-norm (Table D.5) Lipschitz regularization reduce the trivial bound by about two orders of magnitude, and improve generalization performance (Table D.4, Table D.6). Analogously to Figure 5.1, under ∞ -norm regularization, 1-norms of rows are compressed towards the maximum within the same weight matrix (Figure D.1), and under 1-norm regularization, 1-norms of columns are compressed towards the

maximum within the same weight matrix (Figure D.2). This is another illustration of how slackness is optimized away as weight matrices gravitate towards the corners of induced norm balls.

Table D.3. MNIST experiment: Lipschitz bounds for $p = \infty$ norm with various activations.

λ	Polyactivation	K (upper)	\widehat{L} (lower)	K/\widehat{L}
0	(x, x)	35987.51 ± 5478.94	300.86 ± 41.59	119.62
10^{-2}	(x, x)	150.44 ± 1.38	45.61 ± 2.74	3.30
0	$ x $	20648.94 ± 2064.01	248.33 ± 27.08	83.15
10^{-2}	$ x $	152.42 ± 0.24	44.97 ± 3.95	3.39

Table D.4. MNIST experiment: Predictive performance for $p = \infty$ norm with various activations.

λ	Polyactivation	Train NLL	Test NLL	Train Acc.	Test Acc.
0	(x, x)	0.0001 ± 0.0000	0.0875 ± 0.0028	$100.00 \pm 0.00\%$	$98.26 \pm 0.08\%$
10^{-2}	(x, x)	0.0298 ± 0.0010	0.0627 ± 0.0013	$99.59 \pm 0.05\%$	$98.11 \pm 0.08\%$
0	$ x $	0.0001 ± 0.0000	0.0914 ± 0.0057	$100.00 \pm 0.00\%$	$98.29 \pm 0.05\%$
10^{-2}	$ x $	0.0314 ± 0.0006	0.0608 ± 0.0019	$99.50 \pm 0.04\%$	$98.22 \pm 0.09\%$

Table D.5. MNIST experiment: Lipschitz bounds for $p = 1$ norm with various activations.

λ	Activation	K (upper)	\widehat{L} (lower)	K/\widehat{L}
0	$ x $	1405.08 ± 157.65	21.50 ± 4.50	65.36
10^{-2}	$ x $	8.35 ± 0.05	3.76 ± 0.31	2.22
0	$(\tanh, x - \tanh)$	3809.90 ± 1011.06	25.30 ± 1.66	150.61
10^{-2}	$(\tanh, x - \tanh)$	8.02 ± 0.07	3.67 ± 0.30	2.18

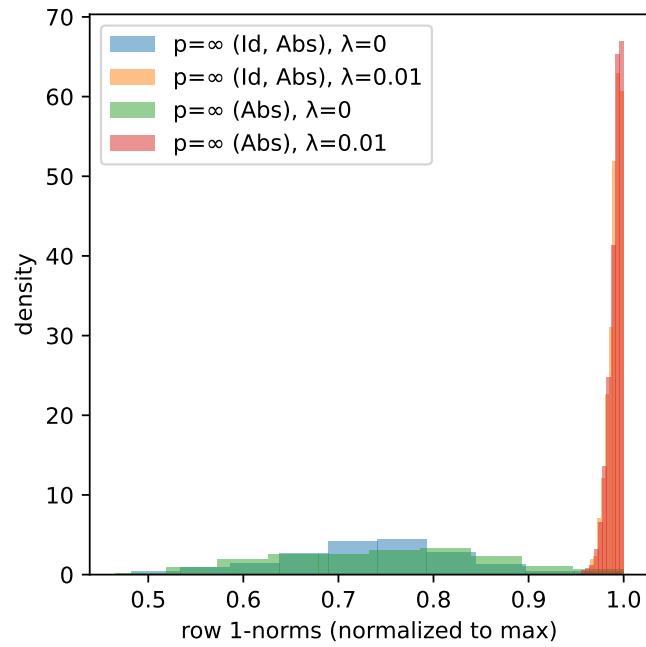


Figure D.1. MNIST experiment: normalized row norms of weight matrices for $p = \infty$ norm (with and without penalty).

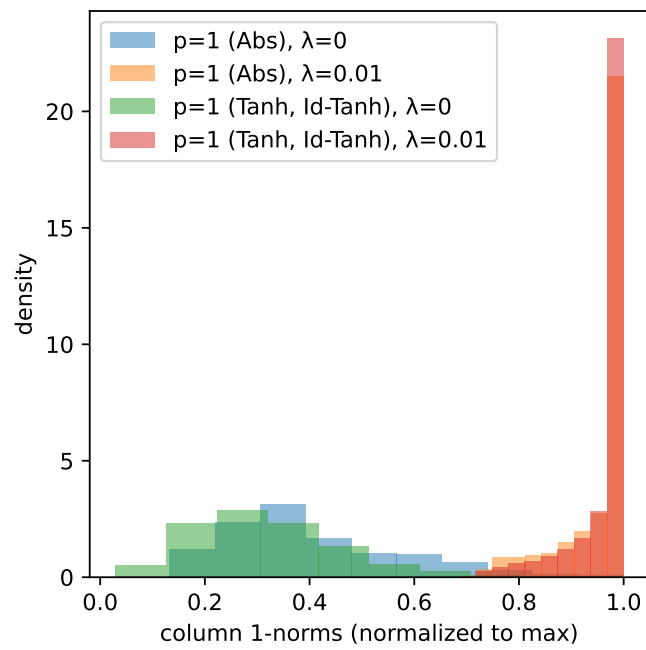


Figure D.2. MNIST experiment: normalized column norms of weight matrices for $p = 1$ norm (with and without penalty).

Table D.6. MNIST experiment: Predictive performance for $p = 1$ norm with various activations.

λ	Activation	Train NLL	Test NLL	Train Acc.	Test Acc.
0	$ x $	0.0001 ± 0.0000	0.0943 ± 0.0060	$100.00 \pm 0.00\%$	$98.25 \pm 0.10\%$
10^{-2}	$ x $	0.0088 ± 0.0003	0.0532 ± 0.0011	$99.98 \pm 0.01\%$	$98.26 \pm 0.08\%$
0	$(\tanh, x - \tanh)$	0.0000 ± 0.0000	0.0876 ± 0.0023	$100.00 \pm 0.00\%$	$98.30 \pm 0.05\%$
10^{-2}	$(\tanh, x - \tanh)$	0.0093 ± 0.0000	0.0524 ± 0.0023	$99.97 \pm 0.00\%$	$98.27 \pm 0.07\%$

Table D.7. MNIST experiment: PGD attack error rates (%) for $p = \infty$ norm with various activations. emp = empirical, cert = certified.

λ	Polyactivation		$\epsilon = 2^{-1}$	$\epsilon = 2^{-2}$	$\epsilon = 2^{-3}$	$\epsilon = 2^{-4}$	$\epsilon = 2^{-5}$
0	(x, x)	emp	99.32 ± 0.26	78.35 ± 1.14	26.26 ± 0.78	7.32 ± 0.19	3.57 ± 0.13
		cert	100.00 ± 0.00				
10^{-2}	(x, x)	emp	95.31 ± 0.67	43.38 ± 1.68	10.60 ± 0.33	4.63 ± 0.23	2.96 ± 0.13
		cert	100.00 ± 0.00	100.00 ± 0.00	100.00 ± 0.00	99.97 ± 0.01	80.88 ± 1.10
0	$ x $	emp	98.88 ± 0.35	73.12 ± 2.18	22.61 ± 1.35	6.61 ± 0.25	3.43 ± 0.13
		cert	100.00 ± 0.00				
10^{-2}	$ x $	emp	93.60 ± 0.98	39.00 ± 0.45	9.65 ± 0.28	4.45 ± 0.21	2.82 ± 0.11
		cert	100.00 ± 0.00	100.00 ± 0.00	100.00 ± 0.00	99.98 ± 0.01	83.14 ± 1.09

Table D.8. MNIST experiment: PGD attack error rates (%) for $p = 1$ norm with various activations. emp = empirical, cert = certified.

λ	Activation		$\epsilon = 2^{-1}$	$\epsilon = 2^{-2}$	$\epsilon = 2^{-3}$	$\epsilon = 2^{-4}$	$\epsilon = 2^{-5}$
0	$ x $	emp	2.03 ± 0.07	1.88 ± 0.12	1.81 ± 0.11	1.79 ± 0.12	1.77 ± 0.11
		cert	100.00 ± 0.00				
10^{-2}	$ x $	emp	2.00 ± 0.13	1.88 ± 0.10	1.81 ± 0.08	1.78 ± 0.08	1.77 ± 0.08
		cert	42.91 ± 0.96	10.02 ± 0.18	4.31 ± 0.06	2.78 ± 0.05	2.20 ± 0.09
0	$x, x - \tanh x$	emp	2.02 ± 0.06	1.85 ± 0.06	1.77 ± 0.06	1.74 ± 0.05	1.72 ± 0.05
		cert	100.00 ± 0.00				
10^{-2}	$x, x - \tanh x$	emp	1.95 ± 0.06	1.83 ± 0.07	1.79 ± 0.08	1.76 ± 0.08	1.75 ± 0.07
		cert	37.83 ± 1.20	9.03 ± 0.30	4.04 ± 0.20	2.65 ± 0.08	2.12 ± 0.06

D.3. Other penalties

Methodology We reproduce the experiment of §5.2 using **Frobenius** norm regularization, a conditioning-promoting modification to the the Frobenius norm (N24, Nenov et al. 2024), and an additive (rather than multiplicative) 2-norm regularization (Y17, Yoshida & Miyato 2017). Both Frobenius and N24 were tuned to assign a weight of 10^{-4} to the Frobenius term. Y17 was tuned with a weight of 10^{-2} .

Results Y17’s adversarial robustness and Lipschitz tightness are within a factor of two of our method, a difference that is within hyperparameter variation (Table D.9, Table D.10). This comparison can be explained by the observation that at the optimum, Y17’s additive penalty and our multiplicative penalty have similar gradients. Our relative contribution is that a multiplicative penalty has a Lipschitz bound interpretation, and we have argued it points toward the most pragmatic way to train Lipschitz neural networks.

Frobenius and N24 boast a trivial bound of 30–40 and a tightness of roughly 2 (Table D.10). Compared to the unregularized network, they yield a smaller and tighter trivial bound, roughly half the PGD failure rate at $\epsilon = 2^{-1}$ (Table C.1), and an empirical Lipschitz lower bound that is about one-fourth as large (Table 5.3). However, their Lipschitz upper bound remains substantially looser than Y17 and our method, and this poor tightness is reflected in over-conservative PGD certificates (Table D.9). This shows that while Frobenius-type regularization has the effect of regularizing the network and may reduce the network’s true Lipschitz constant, this improvement is not conveyed in the trivial Lipschitz upper bound.

Moreover, N24 does not deliver on its promise of regularizing the singular value spectrum of the network’s weight matrices, inducing only a modest rightward shift of the normalized singular value distribution (Figure D.3).

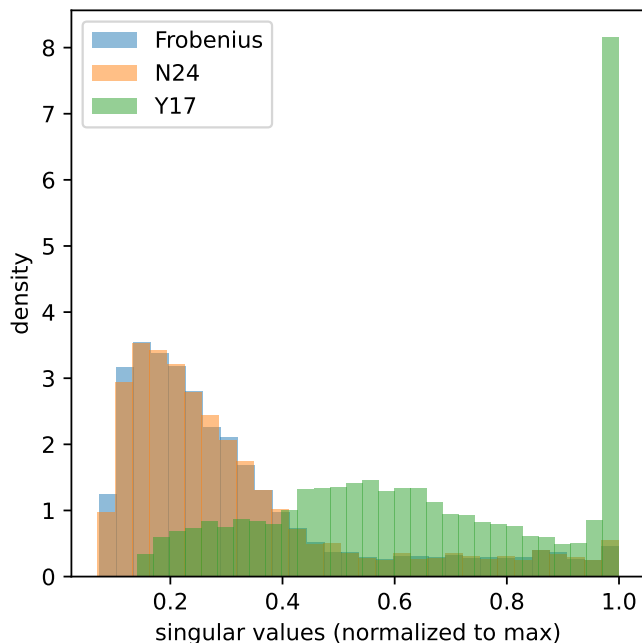


Figure D.3. MNIST experiment: normalized singular values of the weight matrices for alternative regularization methods.

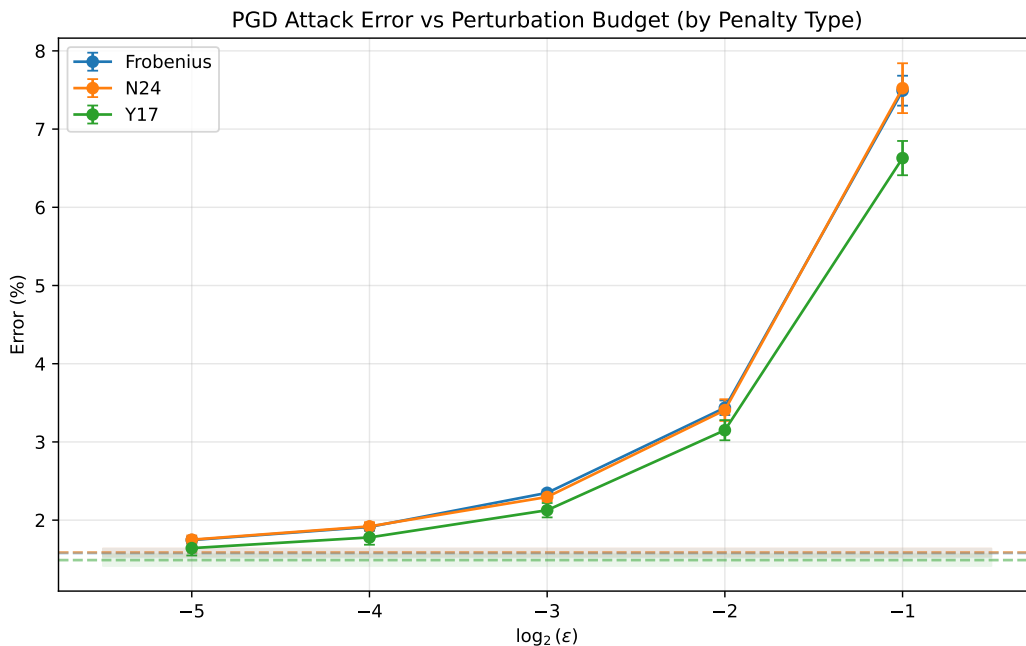


Figure D.4. MNIST experiment: PGD attack error rates for alternative regularization methods.

Table D.9. MNIST experiment: PGD attack error rates (%) for alternative regularization methods.

Penalty		$\epsilon = 2^{-1}$	$\epsilon = 2^{-2}$	$\epsilon = 2^{-3}$	$\epsilon = 2^{-4}$	$\epsilon = 2^{-5}$
Frobenius	emp	7.49 ± 0.19	3.44 ± 0.09	2.35 ± 0.04	1.91 ± 0.05	1.75 ± 0.04
	cert	100.00 ± 0.00	99.47 ± 0.23	30.95 ± 1.96	7.32 ± 0.26	3.42 ± 0.12
N24	emp	7.52 ± 0.32	3.41 ± 0.14	2.30 ± 0.05	1.92 ± 0.05	1.75 ± 0.05
	cert	100.00 ± 0.00	99.22 ± 0.52	30.43 ± 2.89	7.27 ± 0.48	3.38 ± 0.15
Y17	emp	6.63 ± 0.22	3.15 ± 0.13	2.13 ± 0.09	1.78 ± 0.09	1.64 ± 0.09
	cert	86.91 ± 1.62	17.23 ± 0.56	5.43 ± 0.17	2.81 ± 0.11	2.02 ± 0.10

Table D.10. MNIST experiment: Comparison of alternative regularization methods.

Method	K (upper)	\hat{L} (lower)	K/\hat{L}	Train NLL	Test NLL	Test Acc.
Frobenius	35.97 ± 0.88	18.10 ± 1.15	1.99	0.0039 ± 0.0002	0.0495 ± 0.0021	$98.42 \pm 0.06\%$
N24	35.53 ± 1.15	18.19 ± 0.92	1.95	0.0042 ± 0.0003	0.0496 ± 0.0012	$98.41 \pm 0.05\%$
Y17	11.19 ± 0.15	9.21 ± 0.18	1.22	0.0085 ± 0.0002	0.0451 ± 0.0020	$98.51 \pm 0.07\%$

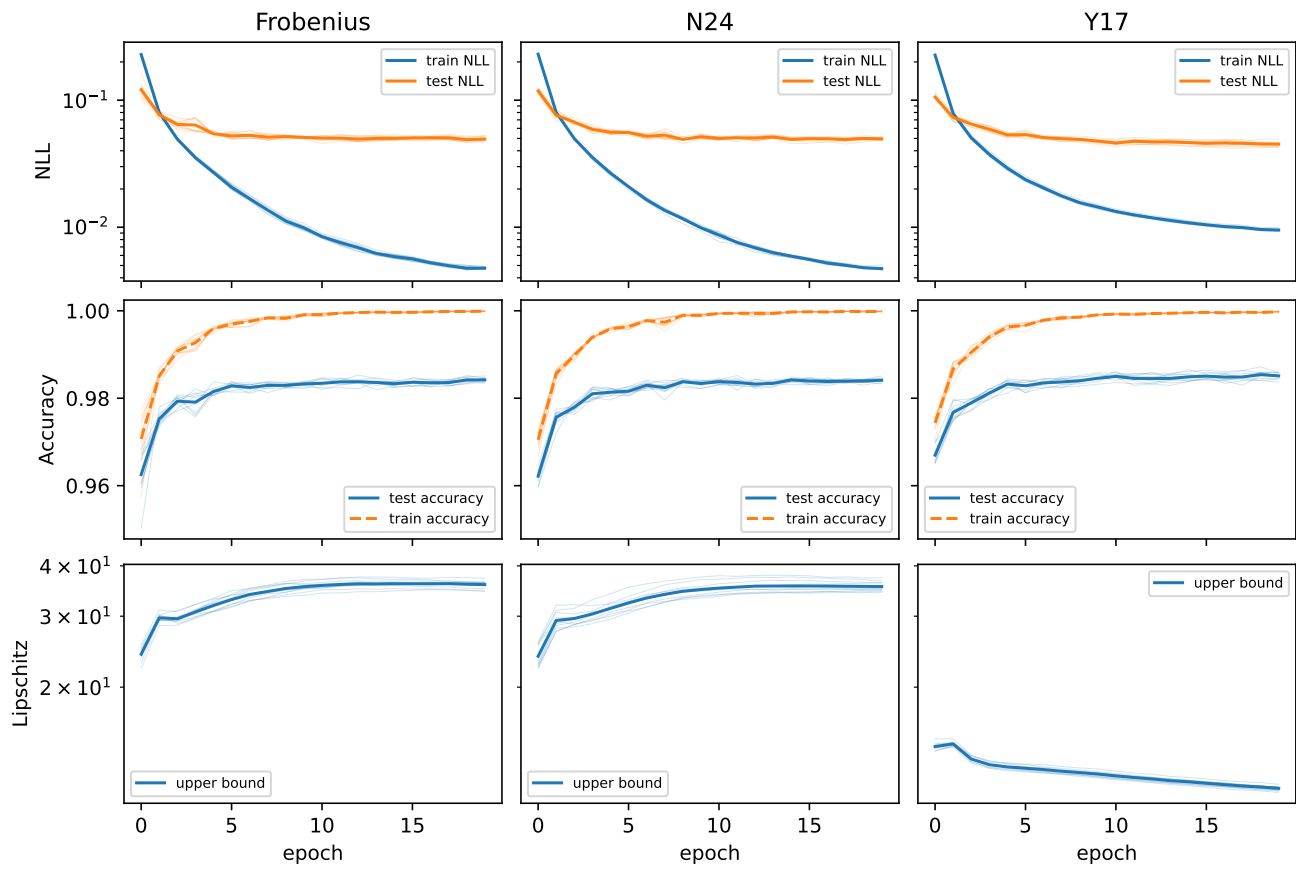


Figure D.5. MNIST experiment: training curves for alternative regularization methods.

D.4. Comparison to a direct parameterization

Methodology Some works maintain a *a priori* Lipschitz constraint while training the network. Granted this objective, is it better to parameterize the Lipschitz cylinder by satisfying a semidefinite program that certifies a ReLU network, by satisfying a trivial bound on a norm-saturating (we choose absolute value as a comparison to ReLU) network?

In order to make a fair comparison, we fix a Lipschitz bound of 0.1 ahead of time and compare the inference performance of **W23**, which takes the SDP route (Wang & Manchester, 2023), with **Ours** parameterization of absolute value networks under the trivial bound, which can be seen as a layer-by-layer decoupling of the SDP constraint. We achieve the same Lipschitz upper bound through a rational parameterization of the induced 2-norm ball of radius 1 (Wang & Manchester, 2023, Proposition 3.3). The set of matrices W satisfying

$$\|W\|_2 \leq 1$$

is parameterized using matrices X, Y by

$$W = 4(I + Z)^{-1} (I - Z) (I + Z)^{-\top} Y^\top, \\ Z = X - X^\top + Y^\top Y.$$

Results Our parameterization achieves better predictive performance than the SDP-based approach, boasting lower training (0.03 vs. 0.12) and test (0.06 vs. 0.13) loss, and higher training (99.64% vs. 98.38%) and test (98.46% vs. 97.78%) accuracy (Table D.11, visualized in Figure D.7).

Our parameterization matches W23’s PGD error rate at the highest radius $\epsilon = 2^{-1}$ and beats it at lower radii (Table D.12, Figure D.6). We attribute this contrast not to a meaningful difference in robustness, but to the fact that $\epsilon \downarrow 0$ reflects a better fit.

This example shows, all else being equal, that the semidefinite constraint is more restrictive than the trivial constraint.

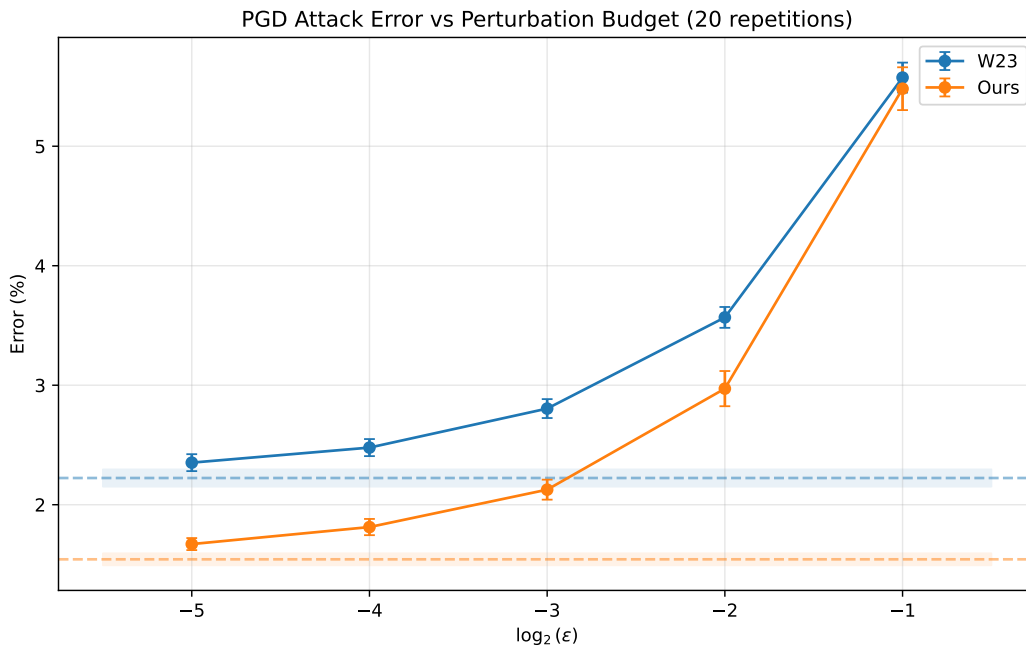


Figure D.6. MNIST experiment: PGD attack error rates for direct parameterization comparison.

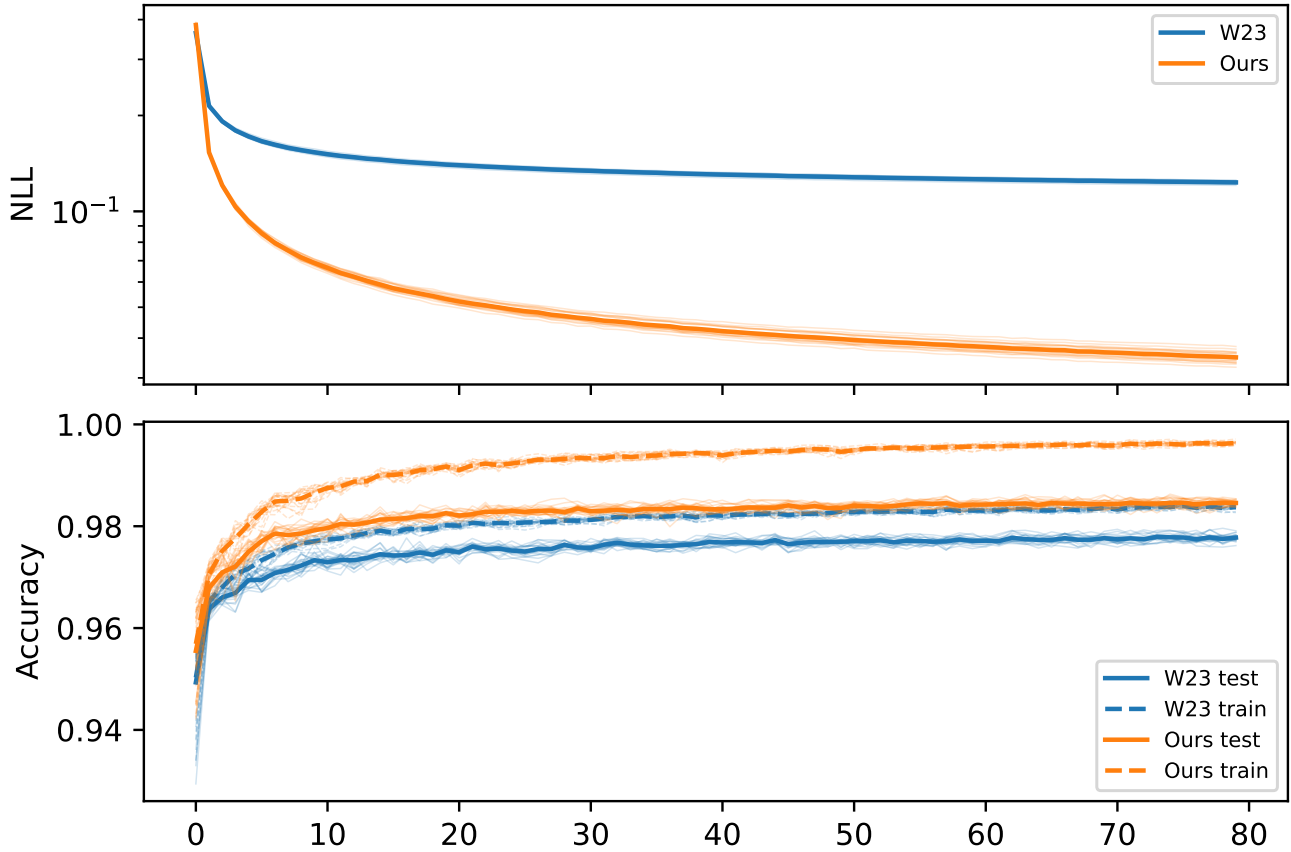


Figure D.7. MNIST experiment: training curves for direct parameterization comparison.

Table D.11. MNIST experiment: Predictive performance for direct parameterization comparison.

Model	Train NLL	Test NLL	Train Acc.	Test Acc.
W23	0.1210 ± 0.0011	0.1320 ± 0.0014	$98.38 \pm 0.05\%$	$97.78 \pm 0.07\%$
Ours	0.0326 ± 0.0013	0.0581 ± 0.0015	$99.64 \pm 0.03\%$	$98.46 \pm 0.05\%$

Table D.12. MNIST experiment: PGD attack error rates (%) for direct parameterization comparison.

Model	$\epsilon = 2^{-1}$	$\epsilon = 2^{-2}$	$\epsilon = 2^{-3}$	$\epsilon = 2^{-4}$	$\epsilon = 2^{-5}$
W23	5.57 ± 0.13	3.57 ± 0.09	2.80 ± 0.08	2.48 ± 0.07	2.35 ± 0.07
Ours	5.48 ± 0.18	2.97 ± 0.15	2.13 ± 0.08	1.81 ± 0.07	1.67 ± 0.05